

1 Article Title

2 Exploration of a European-centered strawberry diversity panel provides markers and candidate genes for 3 the control of fruit quality traits

4
5 **Running title:** GWAS of strawberry quality traits and candidate genes
6

7 Alexandre Prohaska^{1,2}, Pol Rey-Serra¹, Johann Petit¹, Aurélie Petit², Justine Perrotte², Christophe Rothan^{1*},
8 Béatrice Denoyes^{1*}

9 ¹ Univ. Bordeaux, INRAE, UMR BFP, F-33140, Villenave d'Ornon, France.

10 ² Invenio, MIN de Brienne, 110 quai de Paludate, 33000 Bordeaux, France

11
12 * Corresponding authors:
13 **Béatrice Denoyes** <https://orcid.org/0000-0002-0369-9609>
14 Email: beatrice.denoyes@inrae.fr; Phone: +335 57 12 24 60
15 UMR BFP – INRAE, 71 avenue Edouard Bourlaux, 33140 Villenave d'Ornon, France
16 **Christophe Rothan** <https://orcid.org/0000-0002-6831-2823>
17 Email: christophe.rothan@inrae.fr; Phone: +335 57 12 24 60 ;
18 UMR BFP – INRAE, 71 avenue Edouard Bourlaux, 33140 Villenave d'Ornon, France

19
20 Alexandre Prohaska: alexandre.prohaska@gmail.com; <https://orcid.org/0009-0004-0395-7470>
21 Pol Rey-Serra: pol.rey-serra@inrae.fr; <https://orcid.org/0000-0002-3685-2470>
22 Johann Petit: johann.petit@inrae.fr; <https://orcid.org/0000-0002-6746-1755>
23 Aurélie Petit: a.petit@invenio-fl.fr; <https://orcid.org/0000-0003-1577-9072>
24 Justine Perrotte: j.perrotte@invenio-fl.fr
25 Christophe Rothan: christophe.rothan@inrae.fr; <https://orcid.org/0000-0002-6831-2823>
26 Béatrice Denoyes: beatrice.denoyes@inrae.fr; <https://orcid.org/0000-0002-0369-9609>

28

29 **Abstract**

30 Fruit quality traits are major breeding targets in cultivated strawberry (*Fragaria × ananassa*). Taking into
31 account the requirements of both growers and consumers when selecting high quality cultivars is a real
32 challenge. Here, we used an original diversity panel enriched with unique European accessions and the 50K
33 FanaSNP array to highlight the evolution of strawberry diversity over the past 160 years, investigate the
34 molecular basis of 12 major fruit quality traits by GWAS, and provide genetic markers for breeding. Results
35 show that considerable improvements of key breeding targets including fruit weight, firmness, composition
36 and appearance occurred simultaneously in European and American populations. Despite the high genetic
37 diversity of our panel, we observed a drop in nucleotide diversity in certain chromosome regions, revealing
38 the impact of selection. GWAS identified 71 associations with 11 quality traits and, while validating known
39 associations (firmness, sugar), highlighted the predominance of new QTL, demonstrating the value of using
40 untapped genetic resources. Three of the six selective sweeps detected are related to glossiness or skin
41 resistance, two little-studied traits important for fruit attractiveness and, potentially, postharvest shelf-life.
42 Moreover, major QTL for firmness, glossiness, skin resistance and susceptibility to bruising are found within
43 a low diversity region of chromosome 3D. Stringent search for candidate genes underlying QTL uncovered
44 strong candidates for fruit color, firmness, sugar and acid composition, glossiness and skin resistance. Overall,
45 our study provides a potential avenue for extending shelf-life without compromising flavor and color as well
46 as the genetic markers needed to achieve this goal.

47

48 **Keywords:** *Fragaria × ananassa*, strawberry, diversity, fruit quality, GWAS, candidate genes

49

50

51 **Introduction**

52

53 Cultivated strawberry (*Fragaria × ananassa*), the most widely consumed small fruit worldwide, results from
54 spontaneous hybridization in botanical gardens in France in the 18th century between two octoploid ($2n = 8x$
55 = 56) species (*F. chiloensis* and *F. virginiana*) imported from the New World¹. Since then, cultivated
56 strawberry has been continuously improved through the introgression of alleles from wild progenitors
57 creating an admixed population of interspecific hybrid lineages^{2,3,4}. Recurrent hybridization contributed to
58 maintain genetic diversity in the domesticated populations⁴. However, lower genetic diversity and
59 heterozygosity can be observed in highly structured populations, which nevertheless show considerably
60 improved yield, fruit weight and firmness⁵. Current efforts, triggered by consumer demand for sweet and
61 highly-flavored strawberries^{6,7}, are aimed at improving the sensory and nutritional quality of the fruit, for
62 example color⁸ and flavor⁹. Another area for improvement is the extension of the storage period and the
63 reduction of post-harvest rot, both of which are linked to fruit firmness⁷ and little-explored fruit surface
64 properties¹⁰. Several fruit quality traits can be easily manipulated using advanced technology, such as
65 genome editing which has successfully been applied to create new alleles modifying various traits including
66 fruit color, sweetness and aroma^{7,11}. Other complex (e.g. fruit size) and/or little-studied (e.g. fruit glossiness)
67 traits first require elucidation of their genetic architecture. Until recently, following initial studies^{12,13}, the
68 dissection of the genetic control of complex fruit quality traits in *F. × ananassa* has mainly been achieved by
69 mapping Quantitative Trait Locus (QTL) on genetic linkage maps of bi-parental^{14,15,16} or multi-parental¹⁷
70 populations. Causal genetic variants have been identified for several QTL, leading to the design of genetic
71 markers for marker-assisted selection (MAS) of strawberry varieties with, for example, improved fruit
72 color^{8,18} and better aroma⁹.

73

74 Complexity of the allo-octoploid genome of *F. × ananassa*, where up to eight homeo-allelic forms of the same
75 gene can be found¹⁹, has until recently hampered the mapping of QTLs on a given chromosome. Whole
76 genome sequencing of *F. × ananassa*¹ and, more recently, its progenitors²⁰, showed that the four subgenomes
77 of *F. × ananassa* are derived from the diploids *F. vesca* and *F. iinumae* and from two extinct species related
78 to *F. iinumae*²⁰. Genome sequence further enabled the design of a single nucleotide polymorphism (SNP) 50K
79 array with selected chromosome-specific SNPs²¹ allowing the high-resolution mapping of QTLs. A recent
80 breakthrough has been the completion of haplotype-resolved genomes for five genotypes of *F. ×*
81 *ananassa*^{9,22,23,24,25}. These developments make it possible to exploit strawberry diversity through genome
82 wide association studies (GWAS), which scans the genome for significant associations between genetic
83 markers and the trait studied². It thus can help unveil beneficial alleles through the exploration and
84 characterization of large strawberry genetic resources, which display a wide genetic and phenotypic
85 diversity^{4,26,27,28}. So far, GWAS has been done on collections mostly centered on North America strawberry

86 populations^{4,28}, which enabled the discovery of major QTLs controlling fruit weight, firmness, sweetness and
87 aroma^{4,9,28,29,30}. It would certainly benefit from the exploration of other less well-characterized but original
88 populations found in Europe³¹, which is one of the most active strawberry breeding centers⁶.

89

90 In this study, we explored by GWAS the genetic architecture of fruit quality in *F. × ananassa*. To this end, we
91 used the unexploited genetic diversity found in traditional and modern European varieties, in comparison
92 with the better described diversity of North American varieties and some Asian genotypes. Our results are
93 consistent with recent insights into the evolution of modern strawberry varieties and detected major QTL
94 recently described, for fruit firmness for example. Moreover, we detected new QTL for most of the 12 fruit
95 quality traits studied and the underlying candidate genes (CG). An example of this are the QTL and strong CG
96 for the little-explored glossy trait, which underpins the shiny appearance of all modern strawberry varieties
97 and was found to co-localize with a skin resistance trait. Our results therefore highlight the richness of
98 European collections as a source of genetic diversity for strawberry breeding.

99

100 **Results**

101

102 **Population structure and genetic diversity of the diversity panel of cultivated strawberry**

103 We analyzed a germplasm diversity panel comprising 223 accessions of cultivated strawberries (*F. ×*
104 *ananassa*) available at Invenio (South-West France) (Table S1). Unlike the main diversity panels studied to
105 date, where the bulk of the panel was constituted by North American accessions^{4,27}, our panel was mostly
106 composed of European accessions from several countries, with French cultivars being by far the most
107 represented (96 accessions). In addition, the panel comprised representative cultivars from North America
108 including California and Florida, Japan and other breeding programs around the world (Fig. 1A, Table S1).
109 Many cultivars were released between 1990s and nowadays, but the panel also accurately covered the whole
110 modern breeding period (>1950s) and the early stages of strawberry breeding, with cultivars reaching as far
111 as the beginning of the 19th century (Fig. S1). Thirty-two accessions from this panel were common with those
112 from the study by Horvath et al. (2011)³¹. Accessions from the diversity panel were genotyped with the 50K
113 FanaSNP array²¹. A total of 38,120 SNPs was retained after filtering for minor allelic frequency (MAF) (< 5%)
114 and missing data (> 3%).

115 To explore relationships among the 223 accessions, we first evaluated the population structure with
116 STRUCTURE software. We identified three distinct genetic clusters (Fig. 1B, Table S1). Group 1 (G1) includes
117 most of the older European cultivars and their more recent relatives, as well as some old American cultivars
118 (Fig. 1B). This group is hereafter named the Heirloom & related group. Group 2 (G2) clusters essentially
119 European, as well as 14 American cultivars mostly from North-East America (Maryland, New-York and
120 Canada) and three out of five Japanese cultivars (Fig. 1B) and was therefore named the European mixed

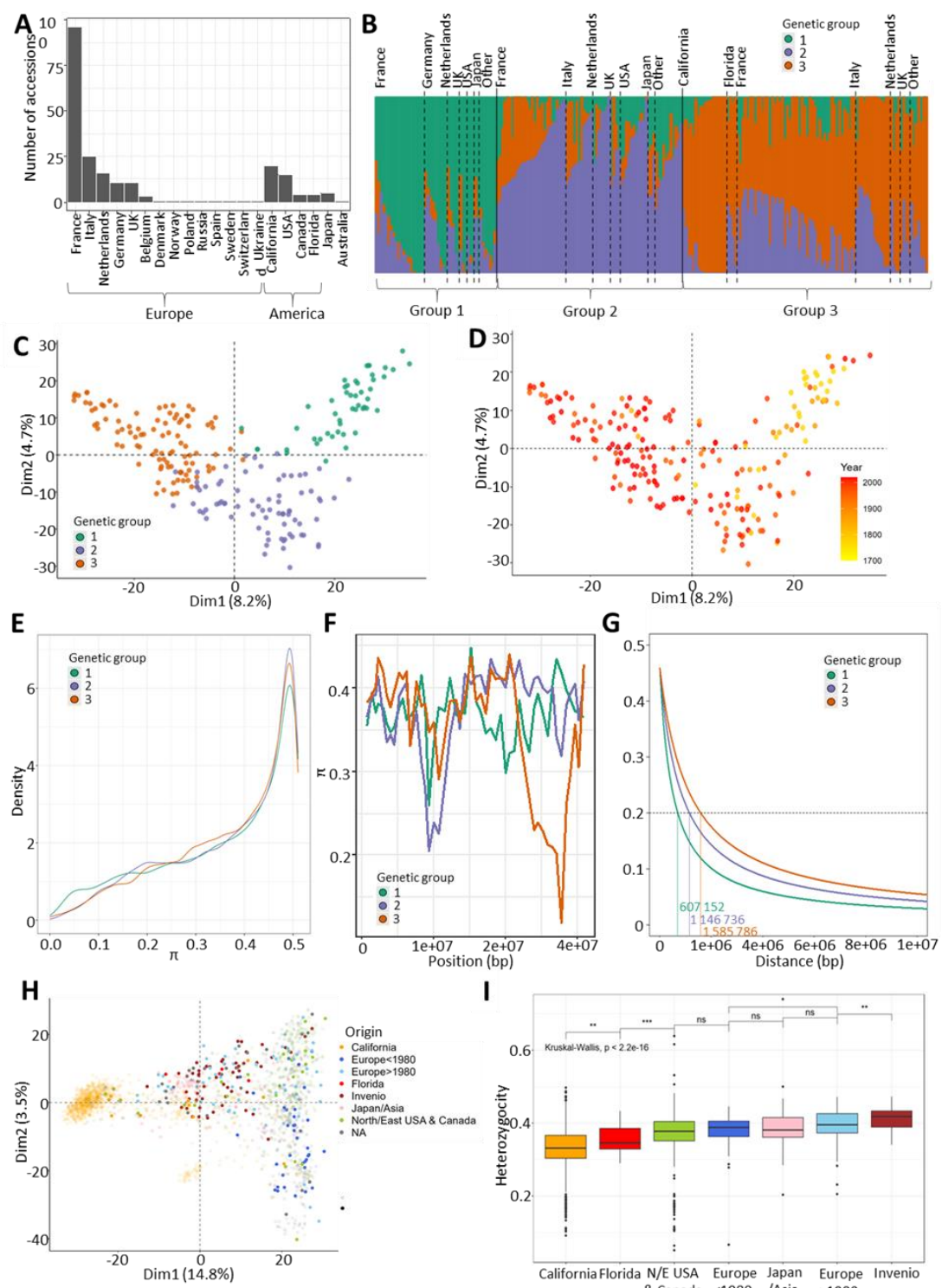
121 group. Californian and Floridian cultivars, together with other European ones, have been identified in group
122 3 (G3) hereafter named the American & European mixed group. A large amount of admixture (< 70%) was
123 observed for each group, with 108 out of 223 accessions split across more than one group, with most of the
124 admixture spread between G2 and G3 (Fig. 1B).

125 To further investigate population structure, we performed principal component analysis (PCA) of the 223
126 accessions using the 38,120 SNP markers (Fig. 1C). The first two dimensions (PC1, PC2) explained 8.2% and
127 4.7% of the structural variance, respectively. The three genetic groups were positioned at each vertex of the
128 crescent shape. PC1 also reflected the temporal separation between G1 and the other two groups when
129 cultivars were displayed according to year of release (Fig. 1D). The phylogenetic analysis (Fig. S2) was
130 consistent with the structure (Fig. 1B) and PCA (Figs 1C, 1D) analyses.

131 Genome-wide comparisons of nucleotide diversity (π) between genetic groups revealed no clear loss of
132 genetic diversity from G1 to G2 and G3 (Fig. 1E). At the chromosome level, the distribution of nucleotide
133 diversity among groups was uneven, with several genomic regions associated with significant enrichment or
134 loss. Of notice, some regions were associated with a sharp reduction in diversity in G2 and/or G3 compared
135 with G1, for example on chromosome 3D, from 23,233 kb to 29,635 kb (Fig. 1F, Fig. S3). Progression towards
136 the most recent American and European cultivars also translated in local augmentation in linkage
137 disequilibrium, where LD (at $r^2 = 0.20$) increased from an average distance of 802,184 bp for G1 to 1,073,213
138 bp for G2 and 1,253,777 bp for G3 (Fig. 1G, Fig. S4).

139 We then combined the SNP data from our diversity panel with those from ⁴ (University of California Davis,
140 UCD panel) and ²⁷ (United States Department of Agriculture, USDA panel) to position our collection in relation
141 with these studies. The PCA of the combined data revealed that the Invenio collection largely overlapped the
142 two USA collections, with the exception of the extreme end of the PC1 corresponding to the UCD program
143 and a small group of genotypes representing probable introgressions of wild accessions into the Californian
144 panel (Fig. 1H, Sup. Fig. 6). The University of Florida (FL) program was less represented in the dataset, and
145 closer to the UCD program on the PCA. Japanese and Asian varieties were located at the center of the
146 crescent. In addition, the PCA highlighted the enrichment of our panel in unique 171 accessions not found in
147 the UCD and USDA panel, thus emphasizing its potential to find new phenotypic diversity for fruit quality
148 traits in cultivated strawberry (Fig. 1H, Fig. S5). Heterozygosity decreased in Californian and Floridian cultivars
149 in comparison to European and Asian cultivars. Interestingly, heterozygosity was significantly higher in
150 cultivars and advanced lines of Invenio and in recent European cultivars (released after 1980) (Fig. 1I).

151



152

153 **Figure 1.** Genetic diversity of the panel. (A) Distribution of the geographical origin of the 223 accessions.
 154 (B) Structure barplot representing each genotype (bars) by its percentage of affiliation to each of the three
 155 genetic groups according to the STRUCTURE analysis. Individuals are sorted by genetic groups and
 156 geographical origins. (C,D) Principal Component Analysis of 38 120 SNP markers. Each accession (dot) is
 157 colored by its genetic group (C) or year of release (D). (E) Nucleotide diversity (π) distributions in windows of
 158 400 kb across each genetic group. (F) π chromosome-wide estimates for each genetic group for 400kb

159 windows across the chromosome 3D. (G) Linkage disequilibrium (LD) decay along chromosome 1A. The
160 dashed line represents the LD decay at $r^2=0.2$. (H) Distribution of the Invenio panel (filled dots) among 1 569
161 genotypes (shaded dots) studied in Hardigan et al. (2021B)⁴ and 539 genotypes studied in Zurn et al. (2022)²⁷
162 (shaded dots) with 3215 SNP markers. Accessions are colored according to geographical/breeding origin. (I)
163 Heterozygosity coefficients across different geographical/breeding origins when combining accessions from
164 the diversity panel and 1569 genotypes from Hardigan et al. (2021b)⁴.
165 Genetic groups 1, 2 and 3 are colored in green, purple and orange, respectively. Groups 1, 2, 3: Heirloom &
166 related, European mixed group and American & European mixed groups, respectively.
167

168 **Fruit quality traits in the diversity panel**

169 A total of 12 fruit quality traits were investigated in the panel of 223 accessions (Table 1). Traits were related
170 to fruit weight (FW); fruit appearance (COL, skin color; UCOL, uniformity of skin color; UFS, uniformity of fruit
171 shape; ACH, position and depth of achenes); firmness (FIRM); composition (TA, titratable acidity; TSS, total
172 soluble solids (Brix units), and BA, the deduced ratio (Brix/TA)); and skin properties (GLOS, glossiness; SR, skin
173 resistance; BRU, bruisedness). Analyses were carried out over two consecutive years, with the exception of
174 the FIRM and SR traits, which were assessed over a single year (Table 1).

175 Most of the traits exhibited a considerable range of variation in the diversity panel, with coefficients of
176 variation ranging from 3.7% for COL to 58.2% for skin resistance. For example, FW (average: 12.5 g) ranged
177 from 1.8 and 32 g. (Table 1). Most traits showed a normal distribution, while SR, GLOS, UFS and BRU showed
178 a skewed distribution (Fig. S6). Nine traits displayed high amount of genotypic variance associated with high
179 broad sense heritability (H^2) ranging from 0.66 (ACH) to 0.98 (FIRM); H^2 of four traits, namely UFS (0.26),
180 UCOL (0.43), BA (0.54) and BRU (0.57), was below 0.6 (Table 1). Few variations of H^2 between groups were
181 observed for FW and FIRM, suggesting that phenotypic variability was equivalent between groups, whereas
182 a strongest decrease in H^2 was observed for GLOS and BRU in G3 (Table 1). A significant interaction between
183 genotype and environment was detected for all the traits for which repeated measurements were available
184 over two years (Table 1), with the effect of environment being strongest for traits related to fruit composition
185 (TSS, TA, BA).

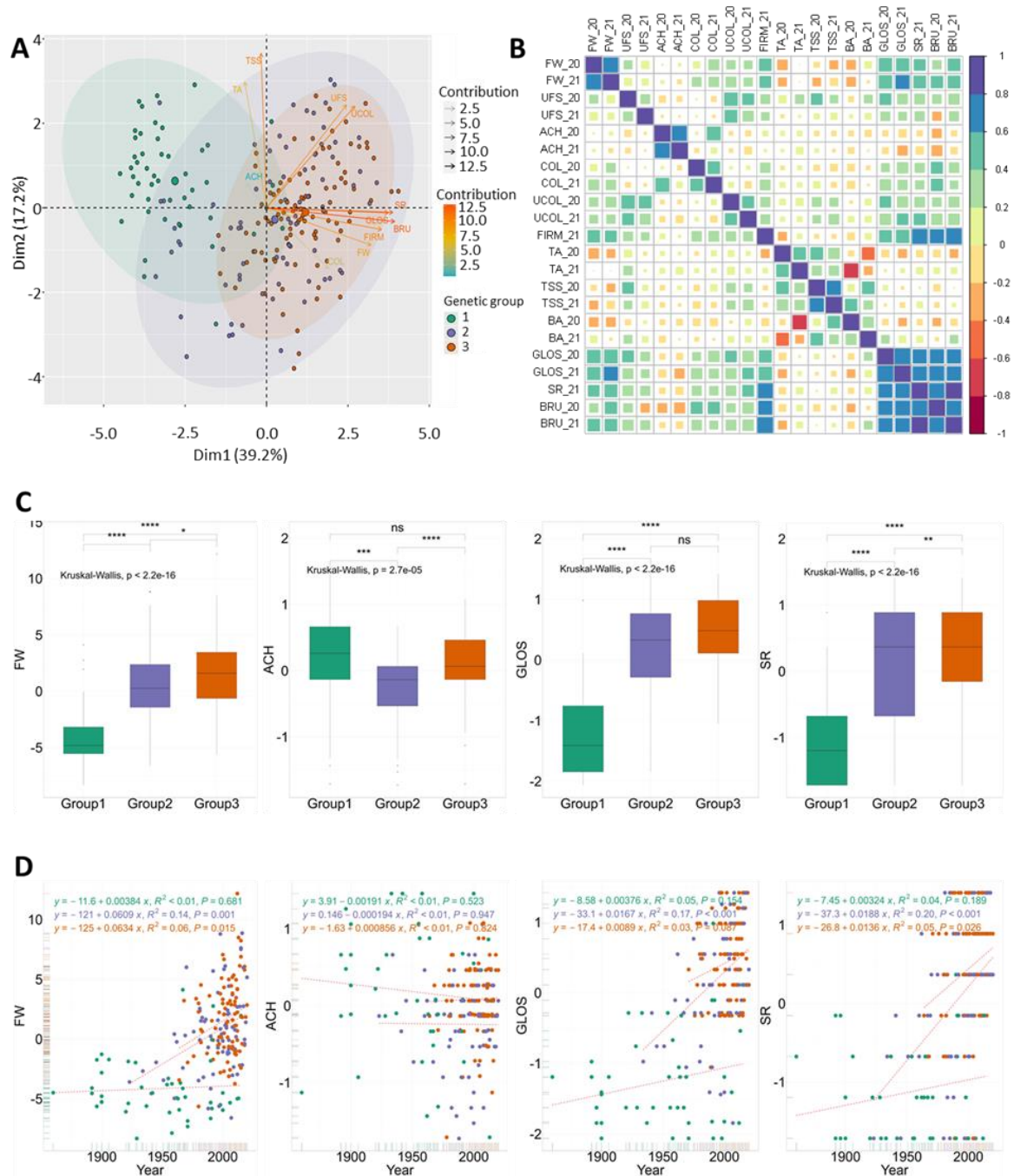
186 To further explore the phenotypes of the diversity panel, we performed a PCA of the 223 accessions using a
187 PCA biplot (Fig. 2A). PC scores revealed that the three genetic groups were distributed differently according
188 to PC1 (39.2%) and PC2 (17.2%) in terms of fruit quality traits. G1 was distinct from G2 and G3 (Fig. 1B).
189 Examination of the loadings of the traits on PC1 further showed that FW, appearance (UFS, UCOL), FIRM and
190 skin properties (GLOS, SR and BRU) traits were responsible for the separation between G1 on one side and
191 G2 and G3 on the other side. TSS, TA and ACH had a very small contribution to the differentiation of the three
192 subpopulations along PC1, and mostly contributed to PC2 and PC3, respectively (Fig. 2A, Fig. S7).
193

194 **Table 1.** Summary statistics of the 12 fruit quality traits evaluated on the diversity panel in 2020 and 2021. n, number of accessions; CV, Coefficient of Variation; H^2 , broad sense heritability; %GE, percentage of genotype-by-environment interactions in the total variance; r^2 structure, structuration of the trait as the coefficient of determination of the linear regression between the trait values and the genetic groups. 20-21 indicates the combined values across two years, 2020 and 2021. ns, not significant genotypic effect.

Trait	Year	n	Range	Mean	σ	CV	H^2	H^2 G1	H^2 G2	H^2 G3	%GE	r^2 structure
Fruit weight (FW, in g)	2020	169	1.8 - 30.9	12.4	5.4	43.6	0.96				-	-
	2021	169	2.0 - 32.0	12.6	5.6	44.5	0.92				-	-
	20-21	169	1.8 - 32.0	12.5	5.5	44.1	0.81	0.71	0.68	0.71	23.4	0.30
Shape uniformity (UFS)	2020	208	1 - 5	2.7	1.3	48.0	-				-	-
	2021	197	1 - 5	3.1	1.3	41.5	-				-	-
	20-21	208	1 - 5	2.9	1.3	44.9	0.26	ns	0.50	ns	-	0.05
Achene position (ACH)	2020	209	1 - 5	3.5	0.8	23.3	-				-	-
	2021	198	1 - 5	3.2	0.9	28.8	-				-	-
	20-21	209	1 - 5	3.4	0.9	26.2	0.66	0.71	0.67	0.60	-	0.08
Skin color (COL)	2020	201	1 - 7	1.2	4.507	3.7	-				-	-
	2021	209	1 - 7.5	1.2	4.535	3.8	-				-	-
	20-21	209	1 - 7.5	1.2	4.522	3.8	0.68	0.77	0.67	0.60	-	0.03
Color uniformity (UCOL)	2020	208	1 - 5	3.0	1.3	42.7	-				-	-
	2021	198	1 - 5	2.8	1.3	47.0	-				-	-
	20-21	208	1 - 5	2.9	1.3	44.9	0.43	ns	0.59	0.32	-	0.10
Firmness (FIRM, in kg/mm)	2020	-	-	-	-	-	-				-	-
	2021	210	1.04 - 0.07	0.433	0.2	40.3	0.98	0.94	0.97	0.95	-	0.44
	20-21	-	-	-	-	-	-				-	-
Titratable acidity (TA, in g / L)	2020	195	0.7 - 2.3	1.4	0.3	20.6	0.83				-	-
	2021	175	0.4 - 2.0	1.2	0.3	24.1	0.91				-	-
	20-21	195	0.4 - 2.3	1.3	0.3	23.1	0.70	ns	0.85	0.82	34.5	0.03
Total soluble solids (TSS, in Brix)	2020	207	3.6 - 11.0	7.1	1.4	19.7	0.92				-	-
	2021	184	3.2 - 11.8	6.9	1.5	22.1	0.94				-	-
	20-21	207	3.2 - 11.8	7.0	1.5	20.9	0.78	0.68	0.83	0.75	30.2	0.04
Brix/acidity ratio (BA)	2020	195	2.9 - 7.9	5.1	1.0	19.9	0.87				-	-
	2021	175	2.1 - 12	5.6	1.5	27.5	0.95				-	-
	20-21	195	2.1 - 12	5.3	1.3	24.8	0.54	ns	0.85	0.51	48.5	0.00
Glossiness (GLOS)	2020	195	1 - 5	3.5	1.2	35.8	-				-	-
	2021	182	1 - 5	3.5	1.1	31.8	-				-	-
	20-21	195	1 - 5	3.5	1.2	33.8	0.77	0.76	0.64	0.43	-	0.48
Skin resistance (SR)	2020	-	-	-	-	-	-				-	-
	2021	210	0 - 3	1.65	1.0	58.2	-				-	0.34
	20-21	-	-	-	-	-	-	-	-	-	-	-
Bruiseness (BRU)	2020	199	1 - 5	2.5	1.3	50.8	-				-	-
	2021	54	0 - 5	1.8	1.0	54.3	-				-	-
	20-21	199	0 - 5	1.9	1.1	55.7	0.57	0.52	0.45	ns	-	0.49

199 200 Correlation analysis of fruit quality trait data collected over 2020 and 2021 (Fig. 2B, Table S2) supported the relationships identified in the PCA biplot (Fig. 2A). GLOS, SR and BRU traits were positively and strongly correlated with each other and with FW and FIRM ($r = 0.51$ to 0.87), indicating the strong potential for directional selection of these traits (Fig. 2A). UFS and UCOL were also highly correlated among them ($r = 0.64$) and, to a lesser extent ($r = 0.35$ and 0.26), with FW. TSS and TA were significantly correlated ($r = 0.45$) but, within groups, the correlation was only significant for G2 ($r = 0.51$) and G3 ($r = 0.47$) groups (Fig. S8). FW also demonstrated significant negative correlations with TSS ($r = -0.21$) and TA ($r = -0.15$) (Fig. 2B; Table S2). No or weak correlations were observed between ACH and other fruit quality traits.

209



210

211 **Figure 2.** Phenotypic variations across the three genetic groups of the panel. (A) Principal Component Analysis
212 of the 2-year BLUP values for 11 traits. (B) Correlations between the 12 traits for each year. (C) Comparisons
213 of 2-year BLUP values for FW, ACH, GLOS and SR among genetic groups. (D) Genetic gains for FW, ACH, GLOS
214 and SR among genetic groups. Genetic groups 1, 2 and 3 are colored in green, purple and orange, respectively.
215 Groups 1, 2, 3: Heirloom & related, European mixed group and American & European mixed groups,
216 respectively. FW, fruit weight; UFS, uniformity of fruit shape; COL, skin color; UCOL, uniformity of skin color;
217 ACH, position and depth of achenes; FIRM, firmness; TA, titratable acidity; TSS, total soluble solids; GLOS,
218 glossiness; SR, skin resistance; BRU, bruisedness.

219

220 Most fruit quality traits have undergone significant phenotypic changes over time, as old varieties have
221 evolved into modern cultivars (Figs 2C, 2D, Fig. S9). Phenotypic values of all fruit quality traits, except BA and
222 COL, were significantly different between the three genetic groups. For example, FW considerably increased
223 during the modern breeding phase, as reflected mainly in trends within G2 and G3 (Figs 2C, 2D) G1 was
224 associated with low FW, dull, soft, low SR and easily wounded skin with uneven color and shape, whereas G3
225 exhibited the highest values for these traits (Fig. 2C, Fig. S9). G2 was equivalent to G3 for UFS and UCOL, TSS
226 and TA, and GLOS; and was in the average of G1 and G3 for FW, FIRM, SR and BRU. Cultivars from G2 displayed
227 more outcropped achenes than the others (Fig. 2C, Fig. S9).

228 These changes are linked to significant genetic gains over time for most fruit quality traits, with the exception
229 of ACH and BA (Fig. 2D, Fig. S10). However, while positive and time-dependent genetic gains were observed
230 within G2 and G3, genetic gains were usually low or nonexistent within G1. For FW, for example, several recent
231 varieties of the G1 showed the same trait values as old ones. A negative, non-significant trend was even
232 observed for TSS and TA, whose values were lower in G2 and G3 than in G1 (Fig. S9). Remarkably, regardless
233 of the TSS and TA reduction in modern varieties compared to old varieties, no significant differences for BA
234 values were observed between groups (Fig. S9).

235

236 **GWAS of fruit quality traits**

237 To reveal the genetic architecture of fruit quality in strawberry, we performed GWAS on the 12 fruit quality
238 traits assessed in the 223 accessions of the strawberry diversity panel using genome-wide SNP markers from
239 the 50K FanaSNP array²¹. The structuration of the population (Figs 2B, 2C) was considered by fitting both
240 kinship and structure as cofactors for GWAS analysis. Detailed Manhattan plots for all 12 traits are shown in
241 Figs 3, 4, Fig. S11. The 71 significant associations with SNP markers are distributed on 51 chromosome regions
242 spread on 23 chromosomes (Table S3).

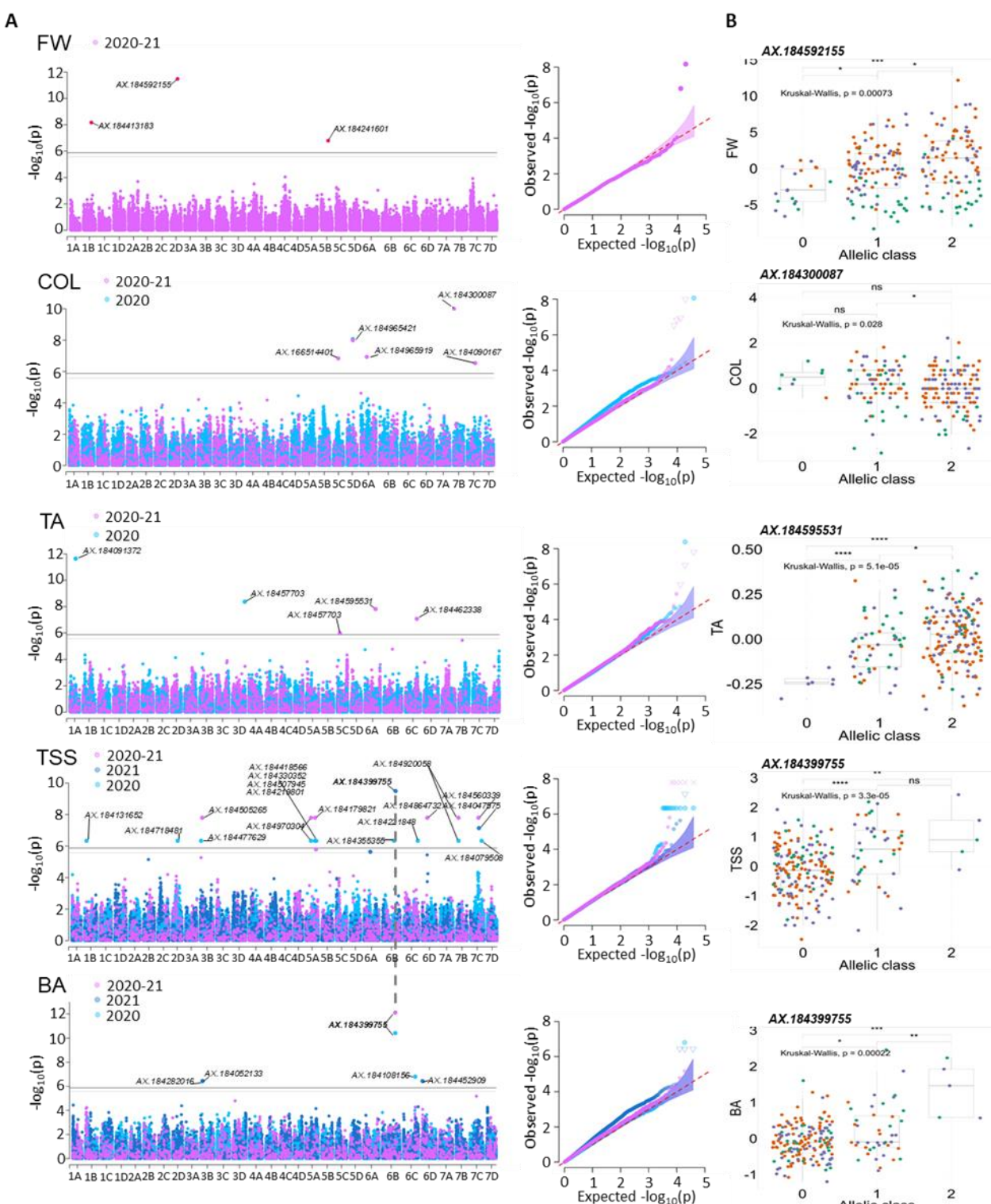
243

244 *Fruit weight and appearance (FW, UFS, COL, UCOL, ACH).*

245 Three significant SNP were identified for FW on chromosome 1B (19,119,571 bp, p-value 6.74E-09), 5B
246 (17,045,086 bp, p-value 1.60E-06) and a highly significant SNP on chromosome 2D (15,565,564 bp, p-value
247 3.27E-12) (Fig. 3A, Table S3). The minor allele of AX-184592155 had a phenotypic variance explained (PVE) of
248 11.8% with an effect of 1.8g on FW (Fig. 3B, Table S3). Sixteen unique significant SNPs were identified for
249 appearance traits, eight for UFS, three for ACH and five for COL (Fig. 3A, Fig. S11, Table S3). No signal was
250 detected for UCOL.

251

252

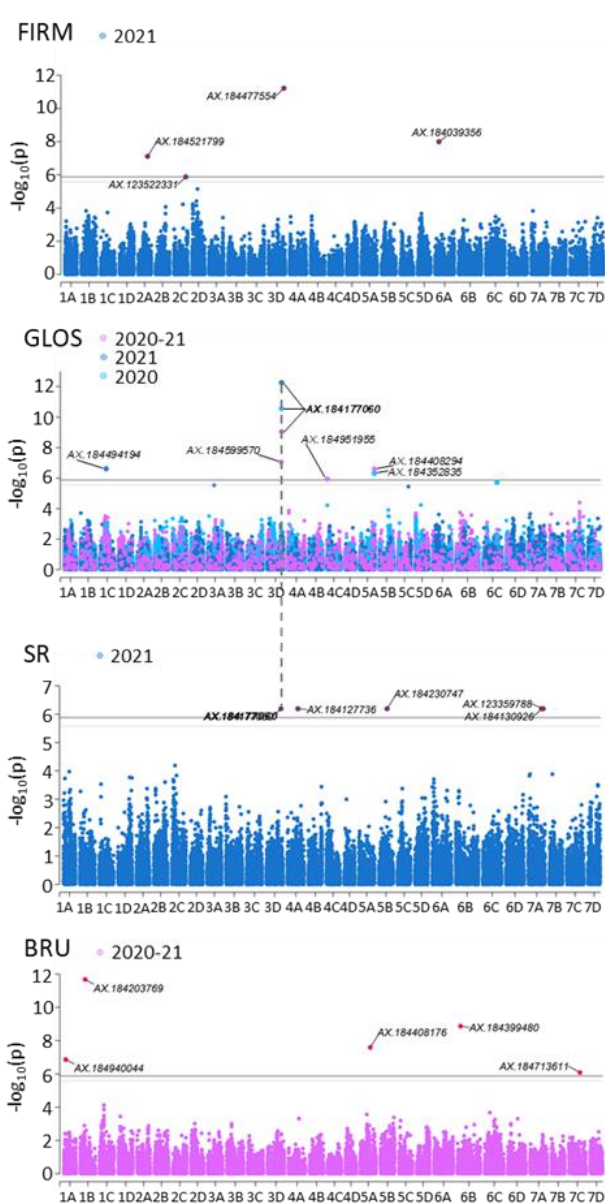


253

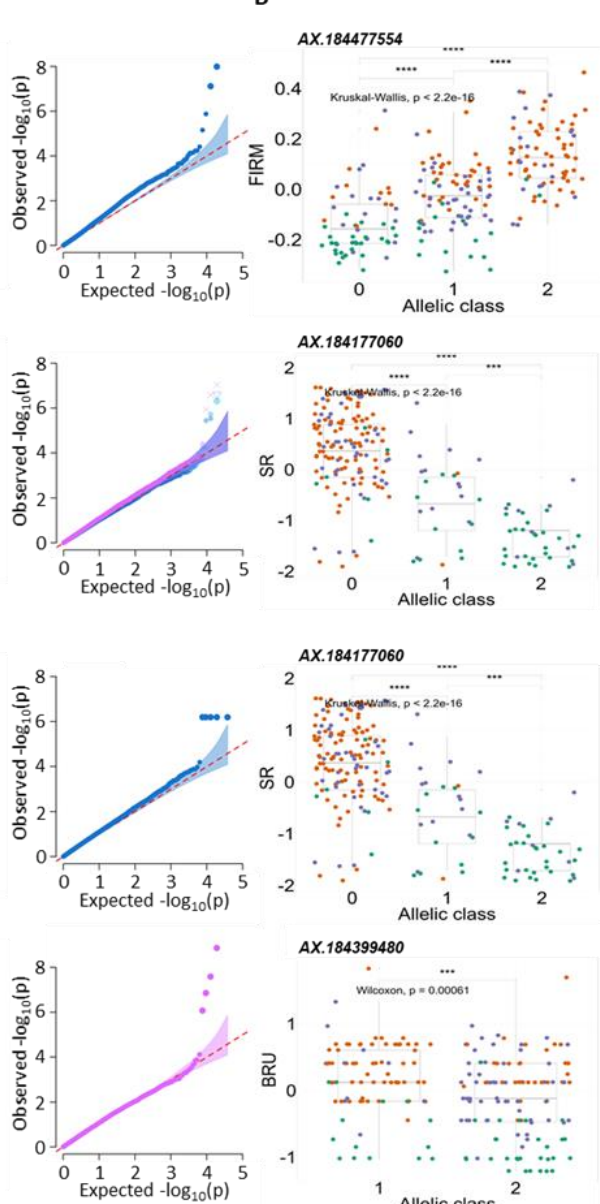
254 **Figure 3.** Genome wide association study of FW, COL, TA, TSS and BA. (A) Manhattan and Q-Q plots for yearly
255 and 2-year BLUP values. (B) Effect of the most significant SNP marker. Genetic groups 1, 2 and 3 are colored
256 in green, purple and orange, respectively. Groups 1, 2, 3: Heirloom & related, European mixed group and
257 American & European mixed groups, respectively. FW, fruit weight; COL, skin color; TA, titratable acidity; TSS,
258 total soluble solids; BA, brix acidity ratio. Marker classes are as follows: 0=AA genotype, 1=AB, and 2=BB
259 genotype according to the Axiom™ Strawberry FanaSNP 50k.

260

A



B



261

262 **Figure 4.** Genome wide association study of FIRM, GLOS, SR and BRU. (A) Manhattan and Q-Q plots for yearly
263 and 2-year BLUP values. (B) Effect of the most significant SNP marker. Genetic groups 1, 2 and 3 are colored
264 in green, purple and orange, respectively. Groups 1, 2, 3: Heirloom & related, European mixed group and
265 American & European mixed groups, respectively. FIRM, firmness; GLOS, glossiness; SR, skin resistance; BRU,
266 bruisedness. Marker classes are as follows: 0=AA genotype, 1=AB, and 2=BB genotype according to the
267 Axiom™ Strawberry FanaSNP 50k.

268

269 *Fruit composition (TA, TSS, BA).*

270 Twenty-seven unique significant SNPs were detected for fruit composition traits, five for TA, 18 for TSS and
271 five for BA (Fig. 3A, Table S3). The SNP AX-184595531 detected for TA on the 2020-2021 combined values
272 (25,621,066 bp, p-value 1.55E-08) was particularly notable for its PVE of 35.5%. Only seven cultivars, all

273 belonging to G2, were unfavorable homozygous for this marker (Fig. 3B). SNPs AX-184091372 on
274 chromosome 1A (13,540,517 bp, p-value 2.30E-12, PVE 17.1%) and AX-184457703 on chromosome 3D
275 (25,621,066 bp, p-value 4.22E-09, PVE 17.9%) were also of particular interest for their PVE and impacting
276 effect on TA in 2021. AX-184399755 was the highest effect SNP for TSS in 2021 on chromosome 6B
277 (31,578,303 bp, p-value 3.24E- 10, PVE 19%) (Fig. 3B). It was also highly significant for BA in 2020 (p-value
278 3.84E- 11, PVE 46.1%) and 2020-2021 combined values (p-value 7.88E- 13, PVE 65.8%) (Fig. 3B). Only five
279 cultivars were favorable homozygous for this marker.

280 Interestingly, on diploid *F. vesca* reference genome (*F. vesca* v4.0.a1³²), the position of SNPs AX-184399755
281 (6B) (10,248,453 bp on diploid) was close (606,797 bp apart) to the position of AX-184864732 (6D)
282 (10,855,248 bp on diploid) indicating that these two TSS QTL could be homoeo-QTL. Same observation was
283 made for SNP AX-184920058 (7B) (20,136,538bp on diploid) and AX-184079508 (7C) (19,687,318 bp on
284 diploid), both being associated to TSS QTL.

285

286 *Fruit firmness and skin properties (FIRM, GLOS, SR, BRU).*

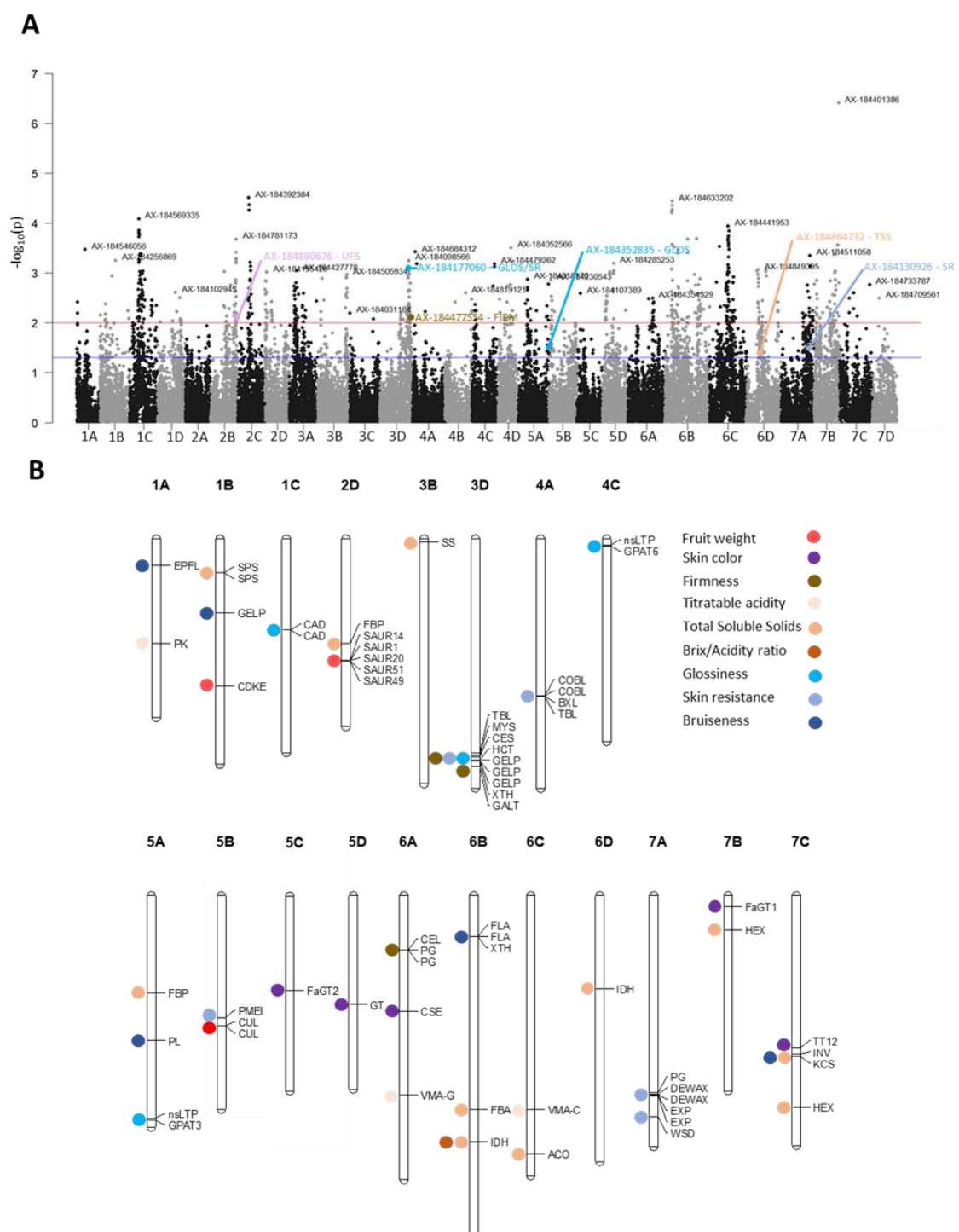
287 Four significant SNPs were detected for FIRM, six for GLOS, five for SR and five for BRU (Fig. 4A, Table S3).
288 The chromosome 3D was of particular interest for these traits as it comprises one highly significant SNP for
289 FIRM (29,275,014 bp, p-value 6.07E- 12, PVE 11.2%) and the highly significant SNP AX-184177060 (27,845,440
290 bp) common to both GLOS (p-value 9.01E- 10, PVE 26.2% on combined values) and SR (p-value 6.45E- 07, PVE
291 8.4%) (Fig. 4B). The latter SNP was detected systematically in 2020, 2021 and 2020-2021 for GLOS with PVE
292 ranging from 26.2% to 28.7%, with a negative effect of the minor allele (-0.7 to -0.8 on 1 to 5 scale). MAF of
293 this SNP was highly reduced towards G3, indicating strong selection of the favorable allele (Fig. 4B). SNPs for
294 BRU bruisedness were detected for the 2020-2021 combined values only.

295

296 **Selective sweep signals during strawberry improvement**

297 We identified markers under selection during strawberry improvement in light of genome scans based on
298 Mahalanobis distance on the whole diversity panel (Fig. 5A) and nucleotide diversity among genetic groups
299 throughout the genome (Fig. 1F, Fig. S3). Six associations were found among candidate selective sweeps
300 based on Mahalanobis distance (Fig. 5A, Table S4), one for UFS, one for FIRM, one for TSS, two for GLOS and
301 one for SR, where SNPs AX-184177060 associated to GLOS and SR, AX-184477554 associated to FIRM, and
302 AX-184864732 associated to TSS, presented a drastic reduction in nucleotide diversity towards modern
303 genotypes (Fig. 1F, Fig. S3, Table S4). For example, in the case of the SR and GLOS SNP marker AX-184177060,
304 the favorable allele is over-represented in the most recent accessions (average year of release 2000),
305 whereas cultivars heterozygous and unfavorably homozygous for the marker were respectively released on
306 average in 1967 and 1947, supporting the fact that the favorable allele has been selected over time. Seven

307 others markers associated to UFS, TA, TSS, GLOS and BRU were also found in genomic regions with substantial
308 depletion in nucleotide diversity in G3 compared to the other groups.
309



310
311 **Figure 5.** Selective sweeps and candidate genes. (A) Selective sweeps as a Manhattan plot of p-values of the
312 genome scan based on Mahalanobis distance. Red and blue lines indicate thresholds at 0.01 and 0.05,
313 respectively; trait associations with a p-value < 0.05 are indicated with colors. (B) Physical mapping of the
314 candidate genes underlying the GWAS of nine traits on the Camarosa genome.

315

316 **Candidate genes were identified for 37 QTL controlling 9 fruit quality traits**

317 Candidate genes (CG) underlying fruit quality QTL were identified within a window of ~400 kb surrounding
 318 the QTL marker. This value, which corresponds to the short-range LD found in the Californian *F. × ananassa*⁴,
 319 is stringent compared to the average LD calculated on the 28 linkage-groups in our diversity panel, which is
 320 932 kb. In chromosome regions harbouring strong QTL of interest and displaying low genetic diversity and
 321 high LD, i.e. the 3D region extending from 23,233 to 29,635 kb (Fig. 1F), we considered much larger intervals
 322 based on LD estimates (up to ~1,382 kb) for 3B and 3D. We excluded two traits (UFS and ACH) from CG
 323 analysis because the molecular pathways underlying these traits are far from being deciphered in strawberry.
 324 No QTL was detected for UCOL. In total, we identified 64 candidate loci for 37 SNP markers associated with
 325 the nine fruit quality traits (Fig. 5B). Table 2 provides names, abbreviations and positions on Camarosa and
 326 Royal Royce genomes of these 64 CG. Their possible functions are indicated in Table S5.

327

328 **Table 2.** Candidate genes underlying nine fruit quality traits. PVE, Phenotypic variance explained (%). Position
 329 Camarosa and Position Royal Royce: physical positions on Camarosa and Royal Royce reference genomes.
 330 Protein encoded by the candidate gene (CG): annotation in the Camarosa genome. CG Position Camarosa
 331 and *F.x ananassa* identity: physical position and identity in the Camarosa genome. * indicate the CG that
 332 were found outside the ~400 kb interval around the SNP marker.

Trait	Chr	PVE	SNP marker	Position Camarosa	Position Royal Royce	Protein encoded by the Candidate Gene (CG)	CG Abbreviation	CG Position Camarosa	F.x ananassa identity	TAIR Arabidopsis homolog	
Fruit weight (FW)	1B	5.5	AX-184413183	19 119 571	15 971 709	cyclin-dependent kinase E-1	CDKE	18 842 135	FxaC_2g34880	AT5G63610.1	
	2D	11.8	AX-184592155	15 565 564	8 801 569	small auxin upregulated RNA 14	SAUR14	15 581 781	FxaC_8g28530	AT4G38840.1	
						small auxin upregulated RNA 1	SAUR1	15 594 644	FxaC_8g28550	AT4G34770.1	
						small auxin upregulated RNA 20	SAUR20	15 611 587	FxaC_8g28590	AT5G18020.1	
						small auxin upregulated RNA 51	SAUR51	15 687 585	FxaC_8g28690	AT1G75580.1	
						small auxin upregulated RNA 49	SAUR49	15 697 093	FxaC_8g28700	AT4G34750.2	
Skin color (COL)	5B	3.6	AX-184241601	17 045 086	10 918 733	cullin	CUL	16 733 799	FxaC_18g25221	AT4G02570.4	
						cullin	CUL	16 708 079	FxaC_18g25150	AT4G02570.4	
Firmness (FIRM)	5C	1.7	AX-166514401	11 987 143	--	anthocyanidin 3-O-glucosyltransferase	FaGT2	12 158 604	FxaC_19g22400	AT5G17050.1	
	5D	3.8-23.4	AX-184965421	14022053	13542145	flavonoid 3-O-glycosyltransferase	GT	14049628	FxaC_20g25430	AT5G54010.1	
	6A	2.6	AX-184965919	14 476 176	21 070 121	caffeoyleshikimate esterase	CSE	14 923 586	FxaC_21g30560	AT1G52760.1	
	7B	3.00986	AX-184300087	1386945	23020879	anthocyanidin 3-O-glucosyltransferase	FaGT1	1422660	FxaC_26g03070	AT5G17050.1	
	7C	9.9	AX-184090167	19 438 028	13 528 856	TT12-like MATE transporter	TT12	19 581 584	FxaC_27g28060	AT4G00350.1	
	3D	11.2	AX-184477554	29 275 014	2 454 715	AGP galactosyltransferase	GALT	29 300 471	FxaC_12g45150	AT4G21060.2	
Titratable acidity (TA)							endotransglucosylase/hydrolase	XTH	28 520 127	FxaC_12g43560	AT3G23730.1
							* cellulose synthase	CES	27 994 587	FxaC_12g42810	AT4G18780.1
	6A	6.3	AX-184039356	7 277 130	27 533 782	cellulase 1	CEL	7 038 578	FxaC_21g15730	AT1G70710.1	
							polygalacturonase	PG	7 048 245	FxaC_21g15750	AT3G07820.1
							polygalacturonase	PG	7 054 511	FxaC_21g15770	AT3G07820.1
	1B	3.6	AX-184131652	4 174 690	1 302 571	pyruvate kinase	PK	13 355 376	FxaC_1g27460	AT2G36580.1	
TSS (Brix)	6A	35.3	AX-184595531	25 621 066	9 172 070	V-type proton ATPase subunit G	VMA-G	25 704 934	FxaC_21g49700	AT3G01390.4	
	6C	6.8	AX-184462338	27 458 040	--	V-type proton ATPase subunit C	VMA-C	27 580 375	FxaC_23g44340	AT1G12840.1	
							fructose-1,6-bisphosphatase, cytosolic	FBP	4 316 703	FxaC_2g09440	AT5G20280.1
	2D	1.41107	AX-184718481	13298291	--	fructose-1,6-bisphosphatase, cytosolic	FBP	4 319 488	FxaC_2g09441	AT5G20280.1	
	3B	0.7	AX-184477629	1 541 393	1 842 542	* starch synthase	SS	453 429	FxaC_10g00830	AT4G18240.1	
	5A	0.9-2.1	AX-184970304	12400711	10544768	fructose-1,6-bisphosphatase, cytosolic	FBP	12546445	FxaC_17g26250	AT1G43670.1	
	6B	1.40326	AX-184355355	27647943	10765128	fructose-bisphosphate aldolase	FBA	27600407	FxaC_22g44640	AT3G52930.1	
	6B	18.9621	AX-184399755	31578303	9217798	isocitrate dehydrogenase [NAD]	IDH	31758475	FxaC_22g50900	AT5G03290.1	
	6C	0.58182	AX-184221848	33293635	29374007	aconitase	ACO	33266087	FxaC_23g56470	AT2G05710.1	
	6D	4.8	AX-184864732	12013420	9512125	isocitrate dehydrogenase [NAD]	IDH	11337718	FxaC_24g21140	AT5G03290.1	
333	7B	1.6-4.0	AX-184920058	4515979	19984301	hexose carrier protein 6	HEX	4480262	FxaC_26g09610	AT5G61520.1	
	7C	7.71803	AX-184047575	20267768	--	alkaline/neutral invertase	INV	20384455	FxaC_27g29380	AT4G09510.1	
	7C	0.5	AX-184079508	26901718	13298291	hexose carrier protein 6	HEX	27292700	FxaC_26g09610	AT5G61520.1	

334

335 Table 2 (to be continued)

Trait	Chr	PVE	SNP marker	Position Camarosa	Position Royal Royce	Protein encoded by the Candidate Gene (CG)	CG Abbreviation	CG Position Camarosa	F.x ananassa identity	TAIR Arabidopsis homolog	
Glossiness (GLOS)	BA ratio	6B	65.8	AX-184399755	31 578 303	9 217 798	isocitrate dehydrogenase [NAD]	IDH	31 758 475	FxaC_22g50900	AT5G03290.1
	1C	17.8	AX-184494194	11 470 545	10 966 861	cinnamyl-alcohol dehydrogenase	CAD	11 709 567	FxaC_3g21930	AT4G39330.1	
						cinnamyl-alcohol dehydrogenase	CAD	11 726 197	FxaC_3g21970	AT4G37970.1	
	3D	4.7-28.7	AX-184599570- AX-184177060	26 901 693- 27 845 440	3 815 908-4 775 280	MYB-SHAQKYF	MYS	27802931	FxaC_12g42500	AT2G38300.1	
						trichome birefringence-like 38	TBL	27585105	FxaC_12g42010	AT1G29050.1	
						* hydroxycinnamoyl-CoA shikimate/quinate	HCT	28432367	FxaC_12g43430	AT5G48930.1	
						* GDSL esterase/lipase	GELP	28471370	FxaC_12g43470	AT1G29670.1	
						* GDSL esterase/lipase	GELP	28475004	FxaC_12g43480	AT1G29670.1	
						* GDSL esterase/lipase	GELP	28478770	FxaC_12g43490	AT1G29670.1	
	4C	3.4	AX-184951955	727143	26073661	non specific Lipid Transport Protein	nsLTP	756662	FxaC_15g01440	AT2G37870.1	
Skin resistance (SR)						glycerol-3-phosphate acyltransferase	GPAT6	901347	FxaC_15g01830	AT2G38110.1	
	5A	4.1-11.1	AX-184408294- AX-184352835	28658239- 28239789	24966878- 25341723	non specific Lipid Transport Protein	nsLTP	28693018	FxaC_17g54360	AT5G64080.1	
						glycerol-3-phosphate acyltransferase	GPAT3	28952583	FxaC_17g54920	AT4G01950.1	
	3D	8.4	AX-184177060	27 845 440	3 815 908	MYB-SHAQKYF 1	MYS	27 802 931	FxaC_12g42500	AT2G38300.1	
						trichome birefringence-like 38	TBL	27 558 105	FxaC_12g42010	AT1G29050.1	
						shikimate/quinate					
						hydroxycinnamoyltransferase	HCT	28 432 367	FxaC_12g43430	AT5G48930.1	
						* GDSL esterase/lipase	GELP	28 471 370	FxaC_12g43470	AT1G29670.1	
						* GDSL esterase/lipase	GELP	28 475 004	FxaC_12g43480	AT1G29670.1	
						* GDSL esterase/lipase	GELP	28 478 770	FxaC_12g43490	AT1G29670.1	
Bruiseness (BRU)	4A	5.4	AX-184127736	20012930	16433479	COBRA-like	COBL	20088406	FxaC_13g38300	AT4G16120.1	
						COBRA-like	COBL	20089498	FxaC_13g38301	AT4G16120.1	
						beta-D-xylosidase	BXL	20219525	FxaC_13g38530	AT5G49360.1	
						trichome birefringence-like 43	TBL	20238095	FxaC_13g38560	AT2G30900.1	
	5B	3.6	AX-184230747	15853776	12173853	pectin methylesterase inhibitor	PMEI	15657184	D=FxaC_18g2343	AT5.1G38610	
	7A	7.3	AX-184130926	25616815	18667225	polygalacturonase	PG	25398299	FxaC_25g46610	AT2G43890.1	
						expansin B2	EXP	25744435	FxaC_25g47360	AT1G65680.1	
						expansin B2	EXP	25766632	FxaC_25g47430	AT1G65680.1	
						decrease was biosynthesis 2	DEWAX	25608061	FxaC_25g47130	AT5G07580.1	
						decrease was biosynthesis 2	DEWAX	25647466	FxaC_25g47200	AT5G07580.1	
336	7A	1.6	AX-123359788	28581204	--	wax ester synthase	WSD	28523042	FxaC_25g3661	AT3G49210.1	
	1A	6.91851	AX-184940044	3531536	--	epidermal patterning factor	EPFL	3396016	FxaC_1g08100	AT3G13898.1	
	1B	6.88666	AX-184203769	9439391	7276991	GDSL lipase	GELP	9476517	FxaC_2g20370	AT2G23540.1	
	5A	4.38749	AX-184408176	18814640	16414924	pectate lyase	PL	18712472	FxaC_17g36850	AT5G09280.1	
	6B	5.48905	AX-184399480	5731875	30532752	fasciclin-like arabinogalactan protein	FLA	5305159	FxaC_22g11190	AT5G06920.1	
						fasciclin-like arabinogalactan protein	FLA	5332088	FxaC_22g11250	AT5G06920.1	
						xyloglucan endotransglucosidase/hydrolase	XTH	5351858	FxaC_22g11330	AT4G03210.1	
337	7C	2.8	AX-184713611	20943204	15149370	3-ketoacyl-CoA synthase 1-like	KCS	20714519	FxaC_27g29940	AT1G01120.1	

338

Discussion

339

340 Genetic and phenotypic shifts in modern strawberry breeding programs

341 Our study sheds light on the genetic and phenotypic shifts that occurred over the last 160 years of strawberry
 342 breeding by analyzing 223 accessions comprising original old and modern European breeding material.
 343 According to our analyses, old strawberry cultivars, which here consist mainly of European cultivars selected
 344 before 1950 and included in the Heirloom & related group (G1), are clearly separated from other genetic
 345 resources (Fig. 1C), in agreement with earlier studies³¹ confirmed in recent papers^{4,33}. For over half a
 346 century³⁴, breeding programs in Western and Southern Europe have made extensive use of Californian
 347 cultivars and, more recently, of Floridan cultivars, which are underrepresented in our study, as progenitors.
 348 As a consequence, our results show the clustering of most European recent cultivars in an American &
 349 European mixed group (G3). The European mixed group (G2), which includes other European cultivars, is

350 likely related to the group previously named Cosmopolitan⁴. However, European from US subpopulations
351 were separated in the USDA panel study, thanks to the large number of US accessions²⁷.
352

353 The nucleotide diversity is overall well conserved among the genetic groups of our panel (Fig. 1E). In contrast,
354 a significant erosion of genetic diversity was observed in highly structured populations^{4,5,28}. We found a more
355 nuanced picture by examining nucleotide diversity at the chromosome level, since it drops dramatically in
356 regions potentially subject to selection pressure (Fig. 1F, Fig. S3). The diminution in both LD and
357 heterozygosity specifically observed in the most recent American cultivars⁴ is likely explained by the gradual
358 closure of Californian and Floridian programs. In contrast, cultivars and advanced lines of Invenio as well as
359 the recent European cultivars released after 1980 display higher heterozygosity values (Fig. 1I). One possible
360 explanation for the high genetic diversity retained in European accessions is that European breeders had to
361 cope with a wide range of breeding targets due to the diversity of cultural practices, markets and consumer
362 preferences found in Europe^{6,35}. High quality strawberry varieties released in Europe therefore had to meet
363 the requirements of both high cultivar performance, e.g. high fruit yield, as in Californian cultivars⁵ and high
364 sensory fruit quality, e.g. high flavor⁶.
365

366 Remarkably, recent studies have shown that despite a loss in genetic diversity, increases in both genetic gain
367 and phenotypic variation were observed in highly structured populations such as those of the Californian
368 breeding programs⁵. In these programs, breeding efforts rapidly led to the improvement of fruit weight and
369 fruit firmness^{5,26,28}, which participated to the so-called Californian green revolution⁵. European breeding
370 programs have benefited from these efforts, as modern American cultivars appear in the pedigree of
371 prominent European cultivars³. Consistently, our results indicate a similar trend towards improved fruit size
372 and firmness, as well as skin glossiness and resistance, in recent European germplasm (Fig. 2C, Fig. S9).
373 Interestingly, we found that TSS and TA values decreased over time in G1 but that the BA ratio kept the same
374 value (Figs S9, S10), in agreement with⁵ who even observed an increase in BA levels, which could partly
375 counterbalance the decrease in fruit sweetness. According to^{5,26,30}, this reflects the antagonism between
376 yield and firmness, on one side, and TSS and TA, on the other side.
377

378 **Novel markers for the selection of fruit quality traits**

379 GWAS is a powerful tool for the detection of SNP markers linked to different traits in strawberry^{9,17,28,30,36,37}.
380 Here, based on a large diversity panel, we detected 71 markers associations to major fruit quality breeding
381 targets. Some of the marker/QTL associations detected confirm published results and, consequently, validate
382 our findings in a different genetic context. For example, our AX-184039356 marker linked to FIRM on 6A is
383 very close to those previously described for fruit firmness^{4,17}. Likewise, our AX-184477629 marker linked to
384 TSS on 3B is in the same chromosome region as the SSC1 QTL controlling soluble solids content³⁰. However,

385 we found in GWAS/QTL published data only a few additional fruit quality QTL located on the same
386 chromosomes as those detected here. Among them are the FW QTL on 5B and the TSS QTL on 5A previously
387 reported³⁸ on the same chromosomes but in different regions. Thus, thanks to the originality of European
388 accessions included in our study, the genetic diversity of the panel allowed us to reveal new QTL and
389 associated SNP markers, even for well-studied fruit quality traits such as FW and TSS.

390

391 In contrast to these well-studied traits, few studies have unveiled the genetic architecture of skin associated
392 traits such as fruit glossiness^{17,39} which is, alongside color, one of the most prominent traits for fruit
393 attractivity to the consumer⁴⁰. Remarkably, among the six associations found among the selective sweeps
394 detected, two were found for GLOS and one for SR (Fig. 5A). Furthermore, by highlighting a ~6,400 kb region
395 on chromosome 3D linked to glossiness, skin resistance and firmness, our results shed a new light on a
396 genomic region under strong breeding pressure (Figs 1F, 5A). Remarkably, among the six associations found
397 among candidate selective sweeps, two were found for GLOS and one for SR. This chromosome region has
398 thus probably played a crucial role in improving the attractivity and post-harvest qualities of strawberries, a
399 feature that is receiving increasing attention in strawberry breeding programs. Information on the position
400 of SNP markers on both Camarosa and Royal Royce genomes will facilitate new studies on fruit quality traits,
401 thus contributing to validate these markers for MAS.

402

403 **Candidate genes**

404

405 *Fruit weight and appearance*

406 Fruit weight (FW) and shape are complex traits. Underlying genes of previously unknown functions have been
407 identified by map-based cloning in species such as tomato⁴¹ and corresponding CG have been detected in
408 several crops⁴². Translation of these findings to strawberry may however prove difficult because of the
409 different ontogenic origin of strawberry, which is an accessory fruit derived from the flower receptacle and
410 not from the ovary. Indeed, our GWAS study did not detect any known gene families linked to fruit weight
411 and shape, but highlighted for FW QTL several CG (*CDKE*, a cluster of five *SAUR*, *CUL*) involved in cell division
412 and expansion processes and their regulation (Table S5).

413

414 Red-colored anthocyanins, which give strawberries their attractive bright red appearance, are flavonoids
415 derived from the phenylpropanoid pathway. In cultivated strawberry, allelic variants of the master regulator
416 *MYB10* belonging to the MBW complex have been shown to be responsible for the white skin-color and red
417 flesh-color^{8,11}. In our GWAS study, we did not detect any previously known color QTL nor CG linked to the
418 MBW complex, probably because white fruit genotypes and flesh-color trait were under-represented in our
419 analysis. However, our diversity panel has enabled us to reveal new skin color QTLs and identify strong CG

420 involved in the successive steps leading to anthocyanin accumulation in strawberry¹¹: (i) anthocyanin
421 biosynthesis; (ii) formation of stabilized anthocyanidin-glucosides; and (iii) transport of anthocyanidin-
422 glucosides for storage in the vacuole. Color CG, which deserve further study, include a gene (*CSE*) encoding
423 shikimate esterase, an enzyme involved in lignin pathway that may compete with anthocyanin biosynthesis
424 for common substrates; several genes encoding glycosyltransferases (*GT*), among which the strawberry
425 *FaGT1* enzyme that has been shown to generate anthocyanidin 3-O-glucosides⁴³ and its homolog *FaGT2*; and
426 a gene encoding a vacuolar flavonoid/H⁺-antiporter (*TT12*) that can actively transport cyanidin-3-O-glucoside
427 to the vacuole⁴⁴.

428

429 *Fruit firmness and composition*

430 Breakdown of the cell wall (CW) is the main mechanism responsible for fruit softening during ripening. CW is
431 mainly constituted by a cellulose-hemicellulose network immersed in a pectin matrix. Strawberry fruit
432 softening involves the pectin-degrading enzymes polygalacturonase (PG) and pectate lyase (PL)⁴⁵. The down-
433 regulation of *PL*⁴⁶ and of *PG*⁴⁷ influences fruit firmness and/or shelf life of strawberry. Many additional
434 proteins are involved in CW modifications e.g. pectin methylesterase (PME) and its inhibitors (PMEI) that
435 control cell adhesion and elasticity through pectin esterification, enzymes of the xyloglucan
436 endotransglycosylase/hydrolase (XTH) family involved in hemicellulose remodelling, cellulases (CEL) that
437 degrade cellulose, and expansins (EXP) that promote CW loosening. Other enzymes such as cellulose
438 synthase (CES) or proteins with ill-defined roles such as arabinogalactan-proteins (AGPs) likely play a role in
439 CW structure and properties. Therefore, considerable variations in fruit firmness can be expected by
440 modulating the activity of enzymes encoded by CG underlying the 3D QTL (*GALT*, *XTH*, *CES*) and 6A (*CEL*, *PG*)
441 QTL. *XTH* and *CES* are strong candidates located at 750 to 1280 kb from the AX-184477554 marker in the
442 well-conserved 3D region while *CEL* and *PG* underly the 6D FIRM QTL previously detected⁴.

443

444 The sugar/acid balance is central for consumers perception of fruit quality¹⁹ and the sugar/acid ratio has been
445 widely adopted as a breeding target⁵. The major soluble sugars that accumulate during fruit ripening are
446 glucose, fructose and sucrose, the concentration of which depends on the cultivar⁴⁸. The major organic acids
447 are malate and especially citrate, which is the predominant organic acid⁴⁸. Their concentrations are stable or
448 decrease during fruit ripening. Fruit sweetness is usually assessed in refractometer (Brix units), which
449 measures total soluble solids (TSS), including sugars and organic acids. Fruit acidity is assessed by titratable
450 acidity (TA), to which citrate contributes most in strawberry. The accumulation in strawberry of soluble sugars
451 and organic acids depends on synthesis in the leaf (source) and long-distance transport of photoassimilates
452 (sucrose, inositol) to the fruit (sink). Photosynthetic sugars are further metabolized in the fruit to produce
453 soluble sugars and organic acids that are then stored in the vacuoles⁴⁹. Our GWAS study identified several CG
454 implicated in the metabolism of sugars, either in the leaves or in the fruit, including *SPS* (1B QTL), *FBP* (2D

455 and 5A QTL), *SS* (3B QTL), *FBA* (6B QTL), and *INV* (7C QTL). The starch synthase (*SS*) is located more than 1 Mb
456 apart from the 3B QTL marker but has been recently identified as a CG for a TSS QTL³⁰. The neutral invertase
457 (*INV*), which underlies the major 7C TSS QTL (PVE 7.7%), is a strong candidate that has been shown to be
458 crucial for glucose and fructose accumulation during ripening in tomato⁵⁰ while a cell wall invertase is
459 responsible for a major TSS QTL in this species⁵¹. Another strong candidate is the hexose transporter (*HEX*)
460 (7B and 7C QTL), which could transport glucose and fructose across the tonoplast, as suggested in grape
461 berries⁵². Furthermore, the *HEX* gene may underlie two possible TSS homoeo-QTL located on chromosomes
462 7B and 7C, respectively.

463

464 Two CG underlying TSS QTL encode enzymes involved in the tricarboxylic acid (TCA) cycle, notably isocitrate
465 dehydrogenase [NAD] (*IDH*) (6B QTL) and aconitase (*ACO*) (6C QTL). TCA is the central metabolic cycle that
466 uses substrates from the glycolysis to produce energy. It fulfills major roles in the fruit, among which the
467 metabolism of citric acid⁵³. While aconitase has been shown to contribute to the regulation of acidity in the
468 citrate-accumulating lemon⁵⁴, we did not detect any TA QTL corresponding to the 6C Brix QTL. Interestingly,
469 *IDH* underlies strong shared QTL for TSS (PVE=19.0) and BA (PVE=65.8) on chromosome 6B. The implication
470 of *IDH* a significant contributor to the TCA cycle, in the sugar/acid balance of strawberry, therefore merits
471 further studies. Moreover, *IDH* is also located at ~ 675 kb from the TSS QTL on chromosome 6D, indicating
472 that it could underlie two TSS homoeo-QTL located on chromosome 6B and 6D, respectively. As previously
473 suggested¹³, the detection of homoeo-QTL could depend on environmental conditions, which vary according
474 to the year of study.

475

476 The CG underlying the 1A TA QTL encodes pyruvate kinase (PK) a crucial enzyme for gluconeogenesis which
477 has already been demonstrated to regulate citric acid metabolism during strawberry fruit ripening⁵³. Two
478 additional CG for the TA QTL located on 6A (PVE 35.3%) and 6C (PVE 6.8%) encode subunits of the V-type
479 proton ATPase (*VMA-G* and *VMA-C*), respectively. Both are strong candidates for the control of fruit acidity,
480 as they are part of a protein complex whose role is to generate a proton gradient across the tonoplast, which
481 is essential to drive the storage of organic acids in the vacuole of fleshy fruits⁵⁵.

482

483 *Skin properties*

484 The outermost wall of the fruit is composed of the cuticle, the epidermis and several layers of sub-epidermal
485 cells⁵⁶. This ill-defined tissue, also called fruit skin⁵⁷, acts as a barrier against water-loss and pathogens and
486 provides protection against mechanical injuries⁵⁸. Its properties depend on epidermal and sub-epidermal cell
487 patterning (cell size and shape) and on the composition and structure of CW and cuticle. To date, the cuticle
488 has been poorly studied in strawberry, except for its composition⁵⁹. Recent studies, in particular in the tomato
489 model, furthered our understanding of the synthesis of cuticle components (wax and cutin polyester,

490 phenolics) and explored the complex interactions between cutin polyesters, CW polysaccharides and
491 phenolics, and their possible contribution to cuticle properties⁵⁶.

492

493 Fruit glossiness is an environment-sensitive trait linked to wax and cutin accumulation on the fruit surface
494 but also to epidermal cell patterning⁶⁰. Among CG identified for GLOS QTL are genes involved in
495 phenylpropanoid pathways (*CAD* in 1C QTL), epidermal patterning (*TBL* in 3D QTL), regulation of wax
496 biosynthesis (*MYS*, 3D QTL), lipid and cutin biosynthesis (*GPAT6*, 4C QTL; *GPAT3*, 5A QTL) and possibly
497 transport of cutin precursors (*nsLTP*, 4C and 5A)^{58,61}. In addition to the *MYS* gene, a transcription factor
498 involved through *DEWAX* in the regulation of the *ECERIFERUM1* (*CER1*) enzyme involved in the biosynthesis
499 of wax alkanes⁶², this region harbors, within ~700 kb of 3D QTL markers, the phenolic pathway *HCT* gene that
500 is essential for cuticle formation⁶³ and, close-by, three *GELP* genes. Several members of the large *GELP* family
501 have been demonstrated to play crucial roles in cutin polymerization (cutin synthase⁶⁴) and in assembly-
502 disassembly of the related polyester suberin⁶⁵. Examination at the Tomato eFP Browser
503 (<http://bar.utoronto.ca>) and TEA-SGN (<https://tea.solgenomics.net>) databases of the expression of the three
504 tomato closest homologs (*Solyc03g005900*, *Solyc02g071610*, *Solyc02g071620*) of the 3D GLOS QTL-linked
505 *GELP* genes indicate that they are strongly expressed in the young fruit, when the cutin synthesis rate is the
506 highest⁶⁰. Furthermore, in the tomato pericarp, their expression is restricted to the outer and inner
507 epidermis. These findings strongly suggest that, in cultivated strawberry, a cluster of genes with likely roles
508 in cuticle formation and structure has been selected in modern varieties for its impact on fruit cuticle-related
509 traits, including GLOS.

510

511 Remarkably, we found that the major skin resistance (SR) QTL, which estimates the fragility of the fruit
512 surface to peel off when a mechanical stress is applied, is shared with the GLOS QTL on 3D. The major 3D
513 FIRM QTL (PVE 11.2%) was also found nearby (at ~1400 kb). Since the FIRM trait was estimated by measuring
514 the force needed to punch a hole in the fruit surface (penetrometer), it can be linked to the properties of the
515 fruit skin. Interestingly, connections between fruit firmness and the cuticle have recently been demonstrated
516 in tomato where changes in cuticle composition and properties are responsible for a major firmness QTL⁶⁶.
517 Altogether, these results suggest that in the 3D conserved region, modifications of fruit surface properties,
518 either due to changes in epidermal cell patterning and/or in cell wall and cuticle properties, have been
519 selected in modern strawberry varieties for their effect on both fruit glossiness, resistance to mechanical
520 damages, and possibly firmness. Other candidates linked to either epidermis patterning (*TBL* on 4A), cell wall
521 modifications (*COBL* and *BXL* on 4A, *PMEI* on 5C, *PG* and *EXP* on 7A) and cuticle formation (*DEWAX*, a target
522 of *MYS*, and *WSD* on 7A) underly the additional SR QTL detected.

523

524 In contrast, none of the QTL detected for fruit bruisedness (BRU), a trait assessed visually, were found to co-
525 localize with either GLOS, SR or FIRM QTL while all these traits are strongly correlated, indicating that the
526 underlying mechanisms are probably different or that the corresponding QTL are below the detection
527 threshold. CW-related GC that may affect cell wall properties (*PL* on 5A, *XTH* on 6B) or cell adhesion of sub-
528 epidermal cells (*FLA* on 6B⁶⁷) merit further investigation, as fruit susceptibility to bruising is essential for post-
529 harvest handling and defense against fruit decay.

530

531 Conclusion

532 In summary, the exploration of untapped genetic resources, including original European cultivars spanning
533 160 years of breeding, has revealed considerable changes in recent decades in the genetic and phenotypic
534 diversity of cultivated strawberry. American cultivars have had a major impact on recent European breeding
535 programs and, therefore, on modern strawberry varieties in Europe. However, our findings also revealed that
536 a considerable, and previously undescribed, genetic diversity can be harnessed for improving fruit quality
537 through breeding. While most fruit quality traits are involved, our study underlines the contribution of little-
538 studied traits related to the fruit surface (glossiness, skin resistance, bruisedness) to the breeding of modern
539 varieties. For these and other traits, the strong CGs underlying the main QTL detected warrant further
540 investigation, for example through additional association studies or functional analyses. From a more applied
541 perspective, the genetic markers highlighted will be used for the selection of improved strawberry varieties
542 with high fruit quality.

543

544 Materials and methods

545

546 Plant materials and experimental design

547 A total of 223 accessions from the historical germplasm collection of Invenio was chosen to constitute the
548 diversity panel. The trial took place in a soilless system, at Douville in the South-West of France (45° 1.2831'
549 N; 0° 37.0198' E, France). The crop management was the one used for commercial semi-early cultivated
550 strawberry in France. The trial was organized in a randomized complete block design of two blocks of four
551 biological replicates each in a 288 m² glass greenhouse in 2020 and 2021. Planting of tray plants occurred
552 around the 15th of December of the previous year.

553

554 Sample preparation and phenotyping

555 Fruits were harvested once per season and evaluated for 12 fruit quality traits: FW, fruit weight; UFS,
556 uniformity of fruit shape; COL, skin color; UCOL, uniformity of skin color; ACH, position of achenes; FIRM,
557 firmness; TA, titratable acidity; TSS, total soluble solids; BA, TSS/TA ratio; GLOS, glossiness; SR, skin resistance;

558 BRU, bruisedness. FW was evaluated as the mean weight of harvested fruits after discarding immature and
559 overripe fruits. UFS, UCOL, ACH as well as GLOS and BRU were visually assessed on 1-5 scales (Table 1) as a
560 single note on a whole strawberry tray (>10 red ripe fruits). COL was evaluated on 4-5 red ripe fruits a 1-8
561 scale based on the strawberry color chart from Ctifl
562 (<http://www.ctifl.fr/Pages/Kiosque/DetailsOuvrage.aspx?IdType=3&idouvrage=833>). FIRM was evaluated
563 on six fruits from each accession with an FTA-GS15 (Güss) penetrometer (5 mm diameter) at 3 mm depth (5
564 mm/s speed, 0.06kg release threshold). SR was evaluated on three fruits per accession on a 1-5 scale by
565 applying an ascending pressure with the extremity of the thumb on the fruit surface. Bruisedness, which
566 represents the susceptibility of the fruit to mechanical damages, was evaluated by visual inspection of the
567 fruits 4 h after harvest. Analyses were performed for two consecutive years except for FIRM and SR traits
568 which were evaluated a single year in 2021. TA and TSS were evaluated from a homogenized pool of a
569 minimum of 10 fruits with a pH-metric titration with sodium hydroxide of 10 g fruit puree and an Atago
570 Handheld (PAL-1) Digital Pocket Refractometer (Atago, Saitama, Japan), respectively.

571

572 **Statistical analysis**

573 Best Unbiased Linear Predictors (BLUPs) for the diversity panel were calculated using a linear mixed model
574 (LMM) from the lme4 R package⁶⁸:

$$575 \quad yijkl = \mu + Gi + Bk + Yl + (G:Y)il + \varepsilon ikl$$

576 where Y/E represented the fixed effects of year/environments, B the fixed effect of blocks, G the random
577 genotypic, GxY/E genotype x year/environment effects and e the residual effects.

578 Variance components for these effects were estimated using restricted maximum likelihood (REML).

579 Broad sense heritability was estimated as follows:

$$580 \quad H^2 = \frac{\sigma^2 G}{\sigma^2 G + \frac{\sigma^2 G:Y}{nyear} + \frac{\sigma^2 e}{nyear \times nrep.year}}$$

581 where genotype (G) variance at the numerator. Random variance components involving year (Y) were
582 divided by the mean number of years (nyear). Other random variance components involving block effects or
583 residuals were divided by the mean number of years times the mean number of replicates per year
584 (nrep.year).

585 Pearson correlation between different traits were calculated using 'cor' function and visualized by 'corrplot'
586 v. 0.92 R package. PCA on all traits was performed using the prcomp function from R core and visualized with
587 fviz_pca function from factoextra v.1.0.7 package or ggplot2 package. The impact of the structure on each
588 variable was assessed by simple regression of the genetic groups on their respective phenotypes.

589

590 **Genotyping**

591 DNA was extracted from young leaves with a CTAB method adapted from Sánchez- Sevilla *et al.*, (2015)³³.
592 Samples were genotyped using Affymetrix® 50K FanaSNP array²¹ in the 'Gentyane' genotyping platform
593 (Clermont-Auvergne-Rhône-Alpes, INRAE, France). SNP calling was processed through Axiom™ Analysis Suite
594 software (v5.1.1.1; Thermo Fisher Scientific, Inc.) following the best practices of the software documentation.
595 Accessions with missing data higher than 3% were removed from analysis. Markers presenting more than 5%
596 of missing data and minor allele frequencies of less than 5% were filtered out.

597

598 **Structure and genetic diversity analysis**

599 We performed a structure population analysis using STRUCTURE (v2.3.4⁶⁹) with 5 runs for a range of K = 2 to
600 10 with 38,120 markers. The burn-in period length was set to 10,000 and 20,000 Markov Chain Monte Carlo
601 (MCMC). The best fitting K was identified with STRUCTURE HARVESTER⁷⁰. Plots were performed using the
602 ggplot2 v.3.3.6 package⁷¹. PCA analyses were performed with PCA function from factorMinerR v.2.7
603 package⁷². Additionally, we included genotypes from Hardigan *et al.*, (2021b)⁴ and Zurn *et al.* (2022)²⁷ to
604 perform PCA using the prcomp function from R core and visualize with fviz_pca_ind function from factoextra
605 v.1.0.7 package or ggplot2 package. We conducted a ML tree with the 233 accessions using IQ-TREE v.2.1.3⁷³
606 with 1000 bootstrap and the TVMe+ASC+R3 model suitable for SNP arrays. Linkage disequilibrium for each
607 chromosome and genetic group was computed using the LDcorSV v.1.3.3 package⁷⁴. Nucleotide diversity
608 among each genetic group was calculated using TASSEL⁷⁵. Finally, we performed principal component
609 analysis-based genome scans to detect markers under selection using the pcadapt package⁷⁶, implementing
610 the pcadapt function with K = 3. Output from genome scans were then compared with nucleotide diversity
611 profiles to search for selective sweeps.

612

613 **Genome-Wide Association Study**

614 The association mapping was performed using GAPIT v.3⁷⁷ using the Camarosa genome physical positions¹
615 with the Bayesian-information and linkage-disequilibrium iteratively nested keyway (BLINK) model⁷⁸. In order
616 to control for confounding effects, the structure was implemented for each trait in two different ways by 1)
617 adding the previously calculated structure parameters as covariates or 2) fitting directly principal
618 components from the principal component analysis using the PCA.total argument. Best models were selected
619 based on genomic inflation factors, λ . The kinship was determined from the SNP data using the VanRaden
620 mean algorithm. The analysis was performed on yearly and across two years Best Linear Unbiased Predictors
621 (BLUPs), using a 5% Bonferroni threshold. Manhattan and Quantile-Quantile plots were plotted using the
622 CMplot R package. Allelic effects for each significant marker were plotted on adjusted means using the
623 ggplot2 R package.

624

625

626 **Conflict of interest statement**

627 The authors declare that there are no conflicts of interest.

628

629 **Author's contributions**

630 BD and AIP conceived and designed the experiments. AIP conducted hands-on experiments and data
631 collection. AuP, JoP and JuP contributed to data collection. AIP, PRS, BD and CR analyzed the data. AIP, BD
632 and CR wrote the original draft. All authors read and approved the final manuscript.

633

634 **Acknowledgements**

635 We thank Sarah Touzani and Eva Bouillon for their help in phenotyping. The project was funded by the
636 Nouvelle-Aquitaine Region and the European Regional Development Fund (ERDF) (REGINA project no.
637 67822110; AgirClim project No. 2018-1R20202); and European Union Horizon 2020 research and innovation
638 program (BreedingValue project No. 101000747; PRIMA-Partnership 2019-2022 Med-Berry project). AIP was
639 supported by the CIFRE (Convention Industrielle de Formation par la Recherche) contract between Invenio
640 (SME, Bordeaux, France) and the INRAE BAP department.

641

642 **Data availability**

643 All relevant data generated or analyzed are included in the manuscript and the supporting materials.

644

645 **References**

646

- 647 1. Edger PP, Poorten TJ, VanBuren R, et al. Origin and evolution of the octoploid strawberry genome. *Nat Genet.* 2019;51(3):541-547. doi:10.1038/s41588-019-0356-4
- 648 2. Whitaker VM, Knapp SJ, Hardigan MA, et al. A roadmap for research in octoploid strawberry. *Hortic Res.* 2020;7:33. doi:10.1038/s41438-020-0252-1
- 649 3. Pincot DDA, Ledda M, Feldmann MJ, et al. Social network analysis of the genealogy of strawberry: retracing the wild roots of heirloom and modern cultivars. *G3 (Bethesda).* 2021;11(3):jkab015. doi:10.1093/g3journal/jkab015
- 650 4. Hardigan MA, Lorant A, Pincot DDA, et al. Unraveling the Complex Hybrid Ancestry and Domestication History of Cultivated Strawberry. *Mol Biol Evol.* 2021b;38(6):2285-2305. doi:10.1093/molbev/msab024
- 651 5. Feldmann MJ, Pincot DDA, Cole GS, and Knapp SJ (2024) Genetic gains underpinning a little-known strawberry Green Revolution. *Nature Communications* (in press).
- 652 6. Senger E, Osorio S, Olbricht K, et al. Towards smart and sustainable development of modern berry
653 cultivars in Europe. *Plant J.* 2022;111(5):1238-1251. doi:10.1111/tpj.15876

660 7. Liu Z, Liang T, Kang C. Molecular bases of strawberry fruit quality traits: advances, challenges, and
661 opportunities. *Plant Physiol.* 2023;kiad376. doi:10.1093/plphys/kiad376

662 8. Castillejo, C. et al. Allelic Variation of MYB10 is the Major Force Controlling Natural Variation of Skin and
663 Flesh Color in Strawberry (*Fragaria* spp.) fruit. *Plant Cell* 32, 3723-3749 (2020).
664 <https://doi.org/10.1105/tpc.20.00474>

665 9. Fan Z, Tieman DM, Knapp SJ, et al. A multi-omics framework reveals strawberry flavor genes and their
666 regulatory elements. *New Phytol.* 2022;236(3):1089-1107. doi:10.1111/nph.18416

667 10. Lara I, Belge B, Goula LF. A focus on the biosynthesis and composition of cuticle in fruits. *J Agric Food
668 Chem.* 2015;63(16):4005-4019. doi:10.1021/acs.jafc.5b00013

669 11. Denoyes B, Prohaska A, Petit J, Rothan C. Deciphering the genetic architecture of fruit color in strawberry.
670 *J Exp Bot.* 2023;erad245. doi:10.1093/jxb/erad245

671 12. Zorrilla-Fontanesi Y, Cabeza A, Domínguez P, et al. Quantitative trait loci and underlying candidate genes
672 controlling agronomical and fruit quality traits in octoploid strawberry (*Fragaria* × *ananassa*). *Theor Appl
673 Genet.* 2011;123(5):755-778. doi:10.1007/s00122-011-1624-6

674 13. Lerceteau-Köhler E, Moing A, Guérin G, et al. Genetic dissection of fruit quality traits in the octoploid
675 cultivated strawberry highlights the role of homoeo-QTL in their control. *Theor Appl Genet.*
676 2012;124(6):1059-1077. doi:10.1007/s00122-011-1769-3

677 14. Labadie M, Vallin G, Petit A, et al. Metabolite Quantitative Trait Loci for Flavonoids Provide New Insights
678 into the Genetic Architecture of Strawberry (*Fragaria* × *ananassa*) Fruit Quality. *J Agric Food Chem.*
679 2020;68(25):6927-6939. doi:10.1021/acs.jafc.0c01855

680 15. Rey-Serra P, Mnejja M, Monfort A. Shape, firmness and fruit quality QTLs shared in two non-related
681 strawberry populations. *Plant Sci.* 2021;311:111010. doi:10.1016/j.plantsci.2021.111010

682 16. Muñoz P, Castillejo C, Gómez JA, et al. QTL analysis for ascorbic acid content in strawberry fruit reveals a
683 complex genetic architecture and association with GDP-L-galactose phosphorylase. *Hortic Res.*
684 2023;10(3):uhad006. Published 2023 Jan 19. doi:10.1093/hr/uhad006

685 17. Cockerton HM, Karlström A, Johnson AW, et al. Genomic Informed Breeding Strategies for Strawberry
686 Yield and Fruit Quality Traits. *Front Plant Sci.* 2021;12:724847. Published 2021 Oct 5.
687 doi:10.3389/fpls.2021.724847

688 18. Labadie M, Vallin G, Potier A, et al. High Resolution Quantitative Trait Locus Mapping and Whole Genome
689 Sequencing Enable the Design of an Anthocyanidin Reductase-Specific Homoeo-Allelic Marker for Fruit
690 Colour Improvement in Octoploid Strawberry (*Fragaria* × *ananassa*). *Front Plant Sci.* 2022;13:869655.
691 doi:10.3389/fpls.2022.869655

692 19. Gaston A, Osorio S, Denoyes B, Rothan C. Applying the Solanaceae Strategies to Strawberry Crop
693 Improvement. *Trends Plant Sci.* 2020;25(2):130-140. doi:10.1016/j.tplants.2019.10.003

694 20. Jin X, Du H, Zhu C, et al. Haplotype-resolved genomes of wild octoploid progenitors illuminate genomic
695 diversifications from wild relatives to cultivated strawberry. *Nat Plants*. 2023;10:1038/s41477-023-
696 01473-2. doi:10.1038/s41477-023-01473-2

697 21. Hardigan MA, Feldmann MJ, Lorant A, et al. Genome Synteny Has Been Conserved Among the Octoploid
698 Progenitors of Cultivated Strawberry Over Millions of Years of Evolution. *Front Plant Sci*. 2020;10:1789.
699 doi:10.3389/fpls.2019.01789

700 22. Hardigan MA, Feldmann MJ, Pincot DDA, et al. 2021a. Blueprint for Phasing and Assembling the Genomes
701 of Heterozygous Polyploids: Application to the Octoploid Genome of Strawberry. *bioRxiv* doi:
702 10.1101/2021.11.03.467115. [Preprint].

703 23. Lee HE, Manivannan A, Lee SY, et al. Chromosome Level Assembly of Homozygous Inbred Line 'Wongyo
704 3115' Facilitates the Construction of a High-Density Linkage Map and Identification of QTLs Associated
705 With Fruit Firmness in Octoploid Strawberry (*Fragaria × ananassa*). *Front Plant Sci*. 2021;12:696229.
706 Published 2021 Jul 14. doi:10.3389/fpls.2021.696229

707 24. Han H, Barbey CR, Fan Z, Verma S, Whitaker VM, Lee S. Telomere-to-Telomere and Haplotype-Phased
708 Genome Assemblies of the Heterozygous Octoploid 'Florida Brilliance' Strawberry (*Fragaria × ananassa*).
709 *bioRxiv* 2022.10.05.509768; doi: <https://doi.org/10.1101/2022.10.05.509768>.

710 25. Mao JX, Wang Y, Wang BT, Li JQ, Zhang C, Zhang WS, Li X, Li J, Zhang JX, Li H, Zhang ZH. High-quality
711 haplotype-resolved genome assembly of cultivated octoploid strawberry. *Horticulture Research*. Volume
712 10, Issue 1, January 2023, uhad002, doi: 10.1093/hr/uhad002

713 26. Hummer K., Bassil NV., Zurn J., Amyotte B. 2022. Phenotypic characterization of a strawberry (*Fragaria*
714 *×ananassa* Duchesne ex Rosier) diversity collection. *Plants, People, Planet*. 5(2):209-224.
715 <https://doi.org/10.1002/ppp3.10316>

716 27. Zurn JD, Hummer KE, Bassil NV. Exploring the diversity and genetic structure of the U.S. National
717 Cultivated Strawberry Collection. *Hortic Res*. 2022;9:uhac125. Published 2022 May 26.
718 doi:10.1093/hr/uhac125

719 28. Fan Z, Whitaker VM. Genomic signatures of strawberry domestication and diversification. *Plant Cell*.
720 Published online December 19, 2023. doi:10.1093/plcell/koad314

721 29. Oh Y, Barbey CR, Chandra S, et al. Genomic Characterization of the Fruity Aroma Gene, FaFAD1, Reveals
722 a Gene Dosage Effect on γ-Decalactone Production in Strawberry (*Fragaria × ananassa*). *Front Plant Sci*.
723 2021;12:639345. doi:10.3389/fpls.2021.639345

724 30. Fan Z, Verma S, Lee H, Jang YJ, Wang Y, Lee S, Whitaker VM. Strawberry soluble solids QTL with inverse
725 effects on yield. *Horticulture Research*, 2024; 11, uhad271, doi.org/10.1093/hr/uhad271

726 31. Horvath A, Sánchez-Sevilla JF, Punelli F, et al. (2011) Structured diversity in octoploid strawberry cultivars:
727 importance of the old European germplasm. *Annals of Applied Biology* 159(3): 358-371
728 doi.org/10.1111/j.1744-7348.2011.00503.x

729 32. Edger PP, VanBuren R, Colle M, et al. Single-molecule sequencing and optical mapping yields an improved
730 genome of woodland strawberry (*Fragaria vesca*) with chromosome-scale contiguity. *Gigascience*.
731 2018;7(2):1-7. doi:10.1093/gigascience/gix124

732 33. Sánchez-Sevilla JF, Horvath A, Botella MA, et al. Diversity Arrays Technology (DArT) Marker Platforms for
733 Diversity Analysis and Linkage Mapping in a Complex Crop, the Octoploid Cultivated Strawberry (*Fragaria*
734 × *ananassa*). *PLoS One*. 2015;10(12):e0144960. Published 2015 Dec 16.
735 doi:10.1371/journal.pone.0144960

736 34. Rosati P. (1993) Recent trends in strawberry production and research: an overview. *Acta Horticulturae*,
737 348, 23–44. DOI:10.17660/ActaHortic.1993.348.1

738 35. Mezzetti, B., Giampieri, F., Zhang, Y.T. & Zhong, C.F. Status of strawberry breeding programs and
739 cultivation systems in Europe and the rest of the world. *J. Berry Res.* 8, 205-221 (2018). DOI:10.3233/JBR-
740 180314

741 36. Davik J, Aaby K, Buti M, et al. Major-effect candidate genes identified in cultivated strawberry
742 (*Fragaria* × *ananassa* Duch.) for ellagic acid deoxyhexoside and pelargonidin-3-O-malonylglucoside
743 biosynthesis, key polyphenolic compounds. *Hortic Res.* 2020;7:125. Published 2020 Aug 1.
744 doi:10.1038/s41438-020-00347-4

745 37. Nagamatsu S, Tsubone M, Wada T, et al. Strawberry fruit shape: quantification by image analysis and QTL
746 detection by genome-wide association analysis. *Breed Sci.* 2021;71(2):167-175. doi:10.1270/jsbbs.19106

747 38. Natarajan S, Hossain MR, Kim HT, et al. ddRAD-seq derived genome-wide SNPs, high density linkage map
748 and QTLs for fruit quality traits in strawberry (*Fragaria* × *ananassa*). *3 Biotech.* 2020;10(8):353.
749 doi:10.1007/s13205-020-02291-5

750 39. Sieczko L., Masny A., Pruski K., Żurawicz E., Mądry W. (2015): Multivariate assessment of cultivars'
751 biodiversity among the Polish strawberry core collection. *Hort. Sci. (Prague)*, 42: 83–93. doi:
752 10.17221/123/2014-HORTSCI

753 40. Lewers KS, Michael J. Newell, Eunhee Park & Yaguang Luo (2020) Consumer preference and
754 physiochemical analyses of fresh strawberries from ten cultivars, *International Journal of Fruit Science*,
755 20:sup2, 733-756, DOI: 10.1080/15538362.2020.1768617

756 41. van der Knaap E, Chakrabarti M, Chu YH, et al. What lies beyond the eye: the molecular mechanisms
757 regulating tomato fruit weight and shape. *Front Plant Sci.* 2014;5:227. Published 2014 May 27.
758 doi:10.3389/fpls.2014.00227

759 42. Wu S, Zhang B, Keyhaninejad N, et al. A common genetic mechanism underlies morphological diversity
760 in fruits and other plant organs. *Nat Commun.* 2018;9(1):4734. Published 2018 Nov 9.
761 doi:10.1038/s41467-018-07216-8

762 43. Griesser M, Hoffmann T, Bellido ML, et al. Redirection of flavonoid biosynthesis through the down-
763 regulation of an anthocyanidin glucosyltransferase in ripening strawberry fruit. *Plant Physiol.*
764 2008;146(4):1528-1539. doi:10.1104/pp.107.114280

765 44. Marinova K, Pourcel L, Weder B, et al. The *Arabidopsis* MATE transporter TT12 acts as a vacuolar
766 flavonoid/H⁺ -antiporter active in proanthocyanidin-accumulating cells of the seed coat. *Plant Cell.*
767 2007;19(6):2023-2038. doi:10.1105/tpc.106.046029

768 45. Moya-León MA, Mattus-Araya E, Herrera R. Molecular Events Occurring During Softening of Strawberry
769 Fruit. *Front Plant Sci.* 2019;10:615. Published 2019 May 15. doi:10.3389/fpls.2019.00615

770 46. Jiménez-Bermúdez S, Redondo-Nevado J, Muñoz-Blanco J, et al. Manipulation of strawberry fruit
771 softening by antisense expression of a pectate lyase gene. *Plant Physiol.* 2002;128(2):751-759.
772 doi:10.1104/pp.010671

773 47. García-Gago JA, Posé S, Muñoz-Blanco J, Quesada MA, Mercado JA. The polygalacturonase FaPG1 gene
774 plays a key role in strawberry fruit softening. *Plant Signal Behav.* 2009;4(8):766-768.
775 doi:10.1104/pp.109.138297

776 48. Moing, A., Renaud, C., Gaudillère, M., Raymond, P., Roudeillac, P., & Denoyes-Rothan, B. (2001).
777 Biochemical Changes during Fruit Development of Four Strawberry Cultivars. *Journal of the American
778 Society for Horticultural Science jashs*, 126(4), 394-403. <https://doi.org/10.21273/JASHS.126.4.394>

779 49. Ruan YL. Sucrose metabolism: gateway to diverse carbon use and sugar signaling. *Annu Rev Plant Biol.*
780 2014;65:33-67. doi:10.1146/annurev-arplant-050213-040251

781 50. Miron D, Petreikov M, Carmi N, et al. Sucrose uptake, invertase localization and gene expression in
782 developing fruit of *Lycopersicon esculentum* and the sucrose-accumulating *Lycopersicon hirsutum*.
783 *Physiol Plant.* 2002;115(1):35-47. doi:10.1034/j.1399-3054.2002.1150104.x

784 51. Fridman E, Carrari F, Liu YS, Fernie AR, Zamir D. Zooming in on a quantitative trait for tomato yield using
785 interspecific introgressions. *Science.* 2004;305(5691):1786-1789. doi:10.1126/science.1101666

786 52. Afoufa-Bastien D, Medici A, Jeauffre J, et al. The *Vitis vinifera* sugar transporter gene family: phylogenetic
787 overview and macroarray expression profiling. *BMC Plant Biol.* 2010;10:245. Published 2010 Nov 12.
788 doi:10.1186/1471-2229-10-245.

789 53. Yang M, Hou G, Peng Y, et al. FaGAPC2/FaPKc2.2 and FaPEPCK reveal differential citric acid metabolism
790 regulation in late development of strawberry fruit. *Front Plant Sci.* 2023;14:1138865. Published 2023 Apr
791 4. doi:10.3389/fpls.2023.1138865

792 54. Shlizerman L, Marsh K, Blumwald E, Sadka A. Iron-shortage-induced increase in citric acid content and
793 reduction of cytosolic aconitase activity in Citrus fruit vesicles and calli. *Physiol Plant.* 2007;131(1):72-79.
794 doi:10.1111/j.1399-3054.2007.00935.x

795 55. Huang XY, Wang CK, Zhao YW, Sun CH, Hu DG. Mechanisms and regulation of organic acid accumulation
796 in plant vacuoles. *Hortic Res.* 2021;8(1):227. Published 2021 Oct 25. doi:10.1038/s41438-021-00702-z

797 56. Reynoud N, Petit J, Bres C, et al. The Complex Architecture of Plant Cuticles and Its Relation to Multiple
798 Biological Functions. *Front Plant Sci.* 2021;12:782773. Published 2021 Dec 10.
799 doi:10.3389/fpls.2021.782773

800 57. Bargel H, Neinhuis C. Tomato (*Lycopersicon esculentum* Mill.) fruit growth and ripening as related to the
801 biomechanical properties of fruit skin and isolated cuticle. *J Exp Bot.* 2005;56(413):1049-1060.
802 doi:10.1093/jxb/eri098

803 58. Petit J, Bres C, Mauxion JP, Bakan B, Rothan C. Breeding for cuticle-associated traits in crop species: traits,
804 targets, and strategies. *J Exp Bot.* 2017;68(19):5369-5387. doi:10.1093/jxb/erx341

805 59. Järvinen R, Kaimainen M, Kallio H. 2010 Cutin composition of selected northern berries and seeds, *Food
806 Chemistry*, Volume 122, Issue 1, pages 137-144. <https://doi.org/10.1016/j.foodchem.2010.02.030>

807 60. Petit J, Bres C, Just D, et al. Analyses of tomato fruit brightness mutants uncover both cutin-deficient and
808 cutin-abundant mutants and a new hypomorphic allele of GDSL lipase. *Plant Physiol.* 2014;164(2):888-
809 906. doi:10.1104/pp.113.232645

810 61. Petit J, Bres C, Mauxion JP, et al. The Glycerol-3-Phosphate Acyltransferase GPAT6 from Tomato Plays a
811 Central Role in Fruit Cutin Biosynthesis. *Plant Physiol.* 2016;171(2):894-913. doi:10.1104/pp.16.00409

812 62. Liu Q, Huang H, Chen Y, et al. Two *Arabidopsis* MYB-SHAQKYF transcription repressors regulate leaf wax
813 biosynthesis via transcriptional suppression on DEWAX. *New Phytol.* 2022;236(6):2115-2130.
814 doi:10.1111/nph.18498

815 63. Kriegshauser L, Knosp S, Grienberger E, et al. Function of the HYDROXYCINNAMOYL-CoA:SHIKIMATE
816 HYDROXYCINNAMOYL TRANSFERASE is evolutionarily conserved in embryophytes. *Plant Cell.*
817 2021;33(5):1472-1491. doi:10.1093/plcell/koab044

818 64. Girard AL, Mounet F, Lemaire-Chamley M, et al. Tomato GDSL1 is required for cutin deposition in the
819 fruit cuticle. *Plant Cell.* 2012;24(7):3119-3134. doi:10.1105/tpc.112.101055

820 65. Ursache R, De Jesus Vieira Teixeira C, Déneraud Tendon V, et al. GDSL-domain proteins have key roles
821 in suberin polymerization and degradation. *Nat Plants.* 2021;7(3):353-364. doi:10.1038/s41477-021-
822 00862-9

823 66. Li R, Sun S, Wang H, et al. FIS1 encodes a GA2-oxidase that regulates fruit firmness in tomato. *Nat
824 Commun.* 2020;11(1):5844. Published 2020 Nov 17. doi:10.1038/s41467-020-19705-w

825 67. Ma Y, Shafee T, Mudiyanselage AM, et al. Distinct functions of FASCILIN-LIKE ARABINOGLALACTAN
826 PROTEINS relate to domain structure [published correction appears in *Plant Physiol.* 2023 Aug
827 3;192(4):3203]. *Plant Physiol.* 2023;192(1):119-132. doi:10.1093/plphys/kiad097

828 68. Bates D, Mächler M, Bolker B, Walker S. Fitting Linear Mixed-Effects Models Using *lme4*. *Journal of
829 Statistical Software.* 2015. 67:1-48. DOI:10.18637/jss.v067.i01

830 69. Pritchard JK, Stephens M, Donnelly P. 2000. Inference of Population Structure Using Multilocus Genotype
831 Data, *Genetics*, 155: 945-959. <https://doi.org/10.1093/genetics/155.2.945>.

832 70. Earl, Dent A. and vonHoldt, Bridgett M. (2011) STRUCTURE HARVESTER: a website and program for
833 visualizing STRUCTURE output and implementing the Evanno method. *Conservation Genetics Resources*
834 DOI: 10.1007/s12686-011-9548-7

835 71. Wickham H (2016). *ggplot2: Elegant Graphics for Data Analysis*. Springer-Verlag New York. ISBN 978-3-
836 319-24277-4. <https://ggplot2.tidyverse.org>.

837 72. Lê S, Josse J, Husson F (2008). "FactoMineR: A Package for Multivariate Analysis." *Journal of Statistical*
838 *Software*, 25(1), 1–18. doi:10.18637/jss.v025.i01

839 73. Minh,B.Q., Schmidt,H.A., hernomor,O. , Schrempf, D., Woodhams,M.D., von Haeseler,A., Lanfear,R.
840 (2020) IQ-TREE 2: New models and efficient methods for phylogenetic inference in the genomic era. *Mol.*
841 *Biol. Evol.*, 37:1530-1534. <https://doi.org/10.1093/molbev/msaa015>

842 74. Mangin, B., Siberchicot, A., Nicolas, S., Doligez, A., This, P., Cierco-Ayrolles, C. (2012). Novel measures of
843 linkage disequilibrium that correct the bias due to population structure and relatedness. *Heredity*, 108
844 (3), 285-291. DOI: 10.1038/hdy.2011.73

845 75. Bradbury PJ., Zhang Z., Kroon DE., Casstevens TM., Ramdoss Y., Buckler ES., TASSEL: software for
846 association mapping of complex traits in diverse samples, *Bioinformatics*, Volume 23, Issue 19, October
847 2007, Pages 2633–2635, <https://doi.org/10.1093/bioinformatics/btm308>

848 76. Luu, K., Bazin, E., & Blum, M. G. (2017). pcadapt: an R package to perform genome scans for selection
849 based on principal component analysis. *Molecular ecology resources*, 17(1), 67-77. doi: 10.1111/1755-
850 0998.12592

851 77. Wang J, Zhang Z. GAPIT Version 3: Boosting Power and Accuracy for Genomic Association and Prediction.
852 *Genomics Proteomics Bioinformatics*. 2021 Aug;19(4):629-640. doi: 10.1016/j.gpb.2021.08.005. Epub
853 2021 Sep 4. PMID: 34492338; PMCID: PMC9121400.

854 78. Huang M, Liu X, Zhou Y, Summers RM, Zhang Z. BLINK: a package for the next level of genome-wide
855 association studies with both individuals and markers in the millions. *Gigascience*. 2019 Feb
856 1;8(2):giy154. doi: 10.1093/gigascience/giy154. PMID: 30535326; PMCID: PMC6365300.

857

858

859

860 **Figure legends**

861

862 **Figure 1. Genetic diversity of the panel.**

863 (A) Distribution of the geographical origin of the 223 accessions.

864 (B) Structure barplot representing each genotype (bars) by its percentage of affiliation to each of the three
865 genetic groups according to the STRUCTURE analysis. Individuals are sorted by genetic groups and
866 geographical origins.

867 (C,D) Principal Component Analysis of 38 120 SNP markers. Each accession (dot) is colored by its genetic
868 group (C) or year of release (D).
869 (E) Nucleotide diversity (π) distributions in windows of 400 kb across each genetic group.
870 (F) π chromosome-wide estimates for each genetic group for 400kb windows across the chromosome 3D.
871 (G) Linkage disequilibrium (LD) decay along chromosome 1A. The dashed line represents the LD decay at
872 $r^2=0.2$.
873 (H) Distribution of the Invenio panel (filled dots) among 1 569 genotypes (shaded dots) studied in Hardigan
874 et al. (2021B)⁴ and 539 genotypes studied in Zurn et al. (2022)²⁷ (shaded dots) with 3215 SNP markers.
875 Accessions are colored according to geographical/breeding origin.
876 (I) Heterozygosity coefficients across different geographical/breeding origins when combining accessions
877 from the diversity panel and 1569 genotypes from Hardigan et al. (2021b)⁴.
878 Genetic groups 1, 2 and 3 are colored in green, purple and orange, respectively. Groups 1, 2, 3: Heirloom &
879 related, European mixed group and American & European mixed groups, respectively.
880

881 **Figure 2. Phenotypic variations across the three genetic groups of the panel.**

882 (A) Principal Component Analysis of the 2-year BLUP values for 11 traits.
883 (B) Correlations between the 12 traits for each year.
884 (C) Comparisons of 2-year BLUP values for FW, ACH, GLOS and SR among genetic groups.
885 (D) Genetic gains for FW, ACH, GLOS and SR among genetic groups.
886 Genetic groups 1, 2 and 3 are colored in green, purple and orange, respectively. Groups 1, 2, 3: Heirloom &
887 related, European mixed group and American & European mixed groups, respectively. FW, fruit weight; UFS,
888 uniformity of fruit shape; COL, skin color; UCOL, uniformity of skin color; ACH, position and depth of achenes;
889 FIRM, firmness; TA, titratable acidity; TSS, total soluble solids; GLOS, glossiness; SR, skin resistance; BRU,
890 bruisedness.
891

892 **Figure 3. Genome wide association study of FW, COL, TA, TSS and BA.**

893 (A) Manhattan and Q-Q plots for yearly and 2-year BLUP values.
894 (B) Effect of the most significant SNP marker.
895 Genetic groups 1, 2 and 3 are colored in green, purple and orange, respectively. Groups 1, 2, 3: Heirloom &
896 related, European mixed group and American & European mixed groups, respectively. FW, fruit weight; COL,
897 skin color; TA, titratable acidity; TSS, total soluble solids; BA, brix acidity ratio. Marker classes are as follows:
898 0=AA genotype, 1=AB, and 2=BB genotype according to the Axiom™ Strawberry FanaSNP 50k.
899

900 **Figure 4. Genome wide association study of FIRM, GLOS, SR and BRU.**

901 (A) Manhattan and Q-Q plots for yearly and 2-year BLUP values.

902 (B) Effect of the most significant SNP marker.
903 Genetic groups 1, 2 and 3 are colored in green, purple and orange, respectively. Groups 1, 2, 3: Heirloom &
904 related, European mixed group and American & European mixed groups, respectively. FIRM, firmness; GLOS,
905 glossiness; SR, skin resistance; BRU, bruisedness. Marker classes are as follows: 0=AA genotype, 1=AB, and
906 2=BB genotype according to the Axiom™ Strawberry FanaSNP 50k.
907

908 **Figure 5. Selective sweeps and candidate genes.**

909 (A) Selective sweeps as a Manhattan plot of p-values of the genome scan based on Mahalanobis distance.
910 Red and blue lines indicate thresholds at 0.01 and 0.05, respectively; trait associations with a p-value < 0.05
911 are indicated with colors.
912 (B) Physical mapping of the candidate genes underlying the GWAS of nine traits on the Camarosa genome.
913

914 **Table legends**

915 **Table 1.** Summary statistics of the 12 fruit quality traits evaluated on the diversity panel in 2020 and 2021. n,
916 number of accessions; CV, Coefficient of Variation; H^2 , broad sense heritability; %GE, percentage of genotype-
917 by-environment interactions in the total variance; r^2 structure, structuration of the trait as the coefficient of
918 determination of the linear regression between the trait values and the genetic groups. 20-21 indicates the
919 combined values across two years, 2020 and 2021. ns, not significant genotypic effect.

920 **Table 2.** Candidate genes underlying nine fruit quality traits. PVE, Phenotypic variance explained (%). Position
921 Camarosa and Position Royal Royce: physical positions on Camarosa and Royal Royce reference genomes.
922 Protein encoded by the candidate gene (CG): annotation in the Camarosa genome. CG Position Camarosa
923 and *F.x ananassa* identity: physical position and identity in the Camarosa genome. * indicate the CG that
924 were found outside the ~400 kb interval around the SNP marker.
925
926

927 **Supplementary data**

928 **Supplementary Figure S1.** Distribution of the year of release for the 223 accessions of the diversity panel.

929 **Supplementary Figure S2.** Phylogenetic tree of the 223 accessions of the diversity panel using the
930 TVMe+ASC+R3 model.

931 **Supplementary Figure S3.** π chromosome-wide estimates for each genetic group for 400kb windows across
932 the octoploid genome.

933 **Supplementary Figure S4.** Linkage disequilibrium (LD) decay along each chromosome of the octoploid
934 genome.

935 **Supplementary Figure S5.** Distribution of the Invenio panel (green dots) among published data.

936 **Supplementary Figure S6.** Distribution of BLUP estimates for the 12 traits.

937 **Supplementary Figure S7.** Principal Component Analysis of the 2-year BLUP values for 11 traits.

938 **Supplementary Figure S8.** Correlations between the 12 traits for each year for each genetic group.

939 **Supplementary Figure S9.** Comparisons of 2-year BLUP values for FIRM, BRU, UFS, UCOL, COL, TA, TSS and

940 BA among genetic groups.

941 **Supplementary Figure S10.** Genetic gains for FIRM, BRU, UFS, UCOL, TA, TSS and BA among genetic groups.

942 **Supplementary Figure S11.** Genome wide association of study of UFS and ACH.

943

944 **Supplementary Table S1.** List of the 223 genotypes.

945 **Supplementary Table S2.** Pearson correlations between 2-year estimated BLUP values for the 12 traits.

946 **Supplementary Table S3.** List of significant trait associations obtained for the GWAS on the 12 traits.

947 **Supplementary Table S4.** Genome scan outputs for the 71 trait associations.

948 **Supplementary Table S5.** Functions and/or possible roles of the 64 candidate genes underlying the trait

949 associations.

950